GasTIPS®

Fall 2005 • Volume 11 • Number 4

TECHNOLOGY DEVELOPMENTS IN NATURAL GAS EXPLORATION, PRODUCTION AND PROCESSING

A Publication of Gas Technology Institute, the U.S. Department of Energy and Hart Energy Publishing, LP

GTI-05/0243

Performance for the long run.

Conductivity Endurance.

Any frac job will boost your production tomorrow. But what about 6 months from now? How do you keep that post-frac flow and maximize total production over the life of the well? That takes **Conductivity Endurance** technology from Halliburton.

It can triple your well's total production—by making your post-fracturing flow rates last much longer. It works by keeping formation fines from clogging the pores in your proppant pack. Minimizing the effects of stress cycling. Keeping the channels open. Keeping the hydrocarbons flowing. Proven effective in hard rock and soft.

Halliburton has the energy to help. To see the proof and learn how Conductivity Endurance can help you finish strong, visit www.halliburton.com.

Unleash the energy.™

HALLIBURTON

Production Optimization

GasTIPS®

Managing Editor
Monique A. Barbee
Hart Energy Publishing, LP

Graphic Design
Melissa Ritchie
Hart Energy Publishing, LP

Editors
Gary Sames
DOE-NETL

Kent Perry
Gas Technology Institute

Subscriber Services
Amy Carruth
custserv@hartenergy.com
Hart Energy Publishing, LP

Publisher
Hart Energy Publishing, LP

CONTENTS

GasTIPS® (ISSN 1078-3954), published four times a year by Hart Energy Publishing, LP, reports on research supported by Gas Technology Institute, the U.S. Department of Energy, and others in the area of natural gas exploration, formation evaluation, drilling and completion, stimulation, production and gas processing.

Subscriptions to ***GasTIPS*** are free of charge to qualified individuals in the domestic natural gas industry and others within the Western Hemisphere. Other international subscriptions are available for $149. Domestic subscriptions for parties outside the natural gas industry are available for $99. Back issues are $25. Send address changes and requests for back issues to Subscriber Services at Hart Energy Publishing, 4545 Post Oak Place, Suite 210, Houston, TX 77027, Fax: (713) 840-0923. Comments and suggestions should be directed to Monique Barbee, ***GasTIPS*** managing editor, at the same address.

Publication Office
Hart Energy Publishing, LP
4545 Post Oak Place, Suite 210
Houston, TX 77027
(713) 993-9320 • FAX:(713) 840-0923

POSTMASTER: Please send address changes to ***GasTIPS***, c/o Hart Energy Publishing, 4545 Post Oak Place, Suite 210, Houston, TX 77027.

Commentary

New Energy Bill Sustains Oil and Gas R&D Efforts in Key Areas

President George W. Bush visited New Mexico's Sandia National Laboratories on Aug. 8 to sign the $14.5 billion Energy Policy Act of 2005. Signing the bill in New Mexico was a nod of appreciation for the efforts of senators Pete Domenici and Jeff Bingaman in moving the bill through Congress. However, the choice of a national lab was also logical as there are a number of initiatives in the bill that support the continuation of ongoing U.S. Department of Energy (DOE) oil and gas research. Specifically, the legislation:

- authorizes the DOE to conduct a research, development and demonstration (R&D) program focused on oil and gas exploration and development, natural gas hydrates, reservoir life extension, oil and gas transportation infrastructure, heavy oil, shale oil, tar sands and related environmental issues;
- instructs the DOE to collect data on marginal well locations, production capacities, reserves and low-pressure gathering systems and recommend measures to enhance their continued operation;
- instructs the DOE to establish a testing facility focused on extended drilling technology at the Rocky Mountain Oilfield Testing Center;
- authorizes the DOE to continue research related to methane hydrates at a funding level that grows from $15 million in 2006 to $50 million in 2010; and
- directs the DOE to conduct an R&D program focused on ultra-deepwater and unconventional oil and gas exploration and production (E&P), including technologies related to safe operations, reducing environmental impact, carbon sequestration and the challenges faced by small producers.

In implementing the last item, the DOE is instructed to contract with a consortium to administer this portion of the program. This consortium may include corporations, trade associations, academic institutions, national labs or other research institutions. The solicitation of proposals from consortium candidates must begin by early November, and a selection must be made within 6 months after that date. The consortium selected will then solicit and select research proposals and funds will be awarded for the development and demonstration of:

- technologies and integrated technology systems for production of ultra-deep water resources;
- technologies for unconventional resources, including advanced coalbed methane, deep drilling, tight gas sands, gas shales and stranded gas; enhanced recovery techniques; and the mitigation of environmental impacts of E&P activities; and
- technologies focused on complex geology, low-pressure reservoirs, unconventional gas reservoirs, tar sands and oil shales (all of these awards will be to consortia representing small producers).

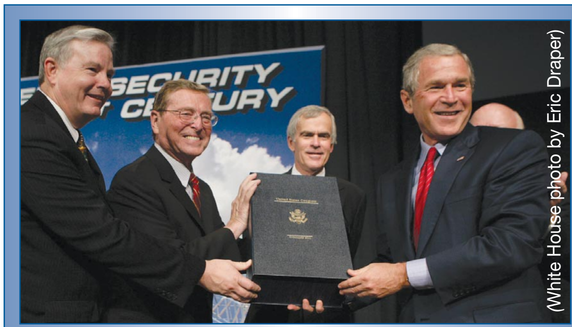

(White House photo by Eric Draper)

President George W. Bush holds the box containing the energy bill after signing the H. R. 6, The Energy Policy Act of 2005. Standing left to right with Bush are Congressman Joe Barton (R, TX), Senator Pete Domenici (R, NM) and Senator Jeff Bingaman (D, NM).

The DOE also is directed to establish advisory committees to provide assistance in planning and direction of R&D programs in the areas related to deepwater and unconventional resources. In particular, the unconventional resource committee is to include a majority of members representing independent producers, along with individuals with extensive operational knowledge of unconventional resource production and individuals broadly representative of the affected interests in unconventional gas and oil resource production.

Funding for the research and its administration by the consortium is to come from Offshore Continental Shelf royalties, in the amount of $50 million per year from 2007 through 2017. The monies collect in an Ultra-Deepwater and Unconventional Natural Gas and Other Petroleum Research Fund where they remain available until expended. The allocation of these funds is also specified: 35% to deepwater, 32.5% to unconventional resources, 7.5% to small producer consortia, and 25% for complementary research and program direction by the DOE. The Energy Policy Act also authorizes the appropriation of an additional $100 million per year to carry out the specified activities.

The president said in signing the bill that "meeting the needs of our growing economy also means expanding our domestic production of oil and natural gas, which are vital fuels for transportation and electricity and manufacturing."

Parts of the energy bill are aimed at ensuring the new supplies of domestic oil and gas are made available as quickly as possible. This issue of *GasTIPS* highlights results from a number of ongoing R&D projects with the same goal in mind. We hope you find this issue informative. ✧

The Editors

Seismic Imaging for Site Selection and Monitoring of Carbon Dioxide Sequestration Part 1— Field Studies

By Iraj A. Salehi and Sherif Gowelly, *Gas Technology Institute*

The Gas Technology Institute with support from Illinois Clean Coal Institute and cooperation of the Illinois State Geological Survey designed and implemented a comprehensive research project aimed at determining the viability of seismic techniques for site selection and monitoring of carbon dioxide sequestration in Illinois coals. Editor's note: This is the first in a two-part series.

As with all greenhouse gas sequestration processes involving injection of greenhouse gases into geologic formations, safety and permanency of the processes require the injected gas to remain within the target zone with no possibility of contaminating water supplies, leaking to unintended zones, or eventually, escaping back into the atmosphere. Therefore, diligent site selection and attentive monitoring are crucial prerequisites for success. Specifically, the host coal seams must be continuous, extend over a large area, occur in structurally closed geometry and be free of faults and displacements.

Advanced seismic technology has proven successful in providing detailed subsurface images of conventional oil and gas reservoirs as well as thicker coal seams. However, Illinois coal seams are shallow and thin, with the thickness rarely exceeding 10ft. The first objective of this project was to establish viability of seismic imaging of thin coal seams in Illinois. This was investigated in a series of seismic data acquisitions including surface seismic, vertical seismic profiling and cross-well seismic imaging. The data proved thin coal seams can reliably be mapped by properly designed seismic surveys.

The second project objective was to verify viability of time-lapse (4-D) seismic as a monitoring tool for potential carbon dioxide

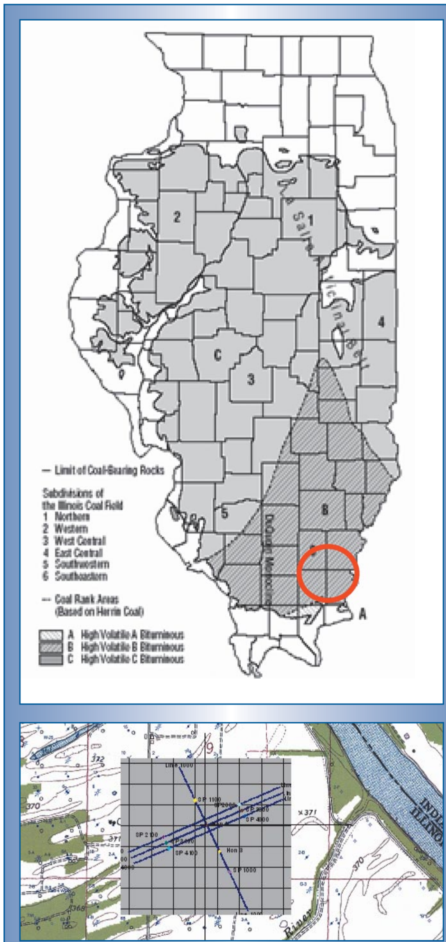

Figure 1. Location of seismic lines and survey wells at the Illinois State Geological Survey pilot site.

(CO_2) sequestration projects in coal seams of Illinois. Although 4-D seismic has proven successful in monitoring gas movements in conventional reservoirs, because of the intrinsic properties of coal seams, it is not known whether the technique is viable for mapping the gas front in coals. In pursuing this objective, a number of elaborate laboratory measurements of acoustic velocity in gas- and water-saturated coal samples were carried out. Results showed the magnitude of velocity changes resulting from addition of a gas phase into water-saturated coal is large enough to render the time-lapse seismic technique useful for monitoring the position of the injected gas front.

Results from this project are presented in two parts. Part one describes results from field seismic surveys and part two, which will appear in the *GasTIPS* Winter 2006 issue, will discuss results from laboratory measurements.

Introduction

Site selection for injection of greenhouse gases into geologic formations is a non-trivial task. The target zone must be contained between impermeable overlying and underlying beds, structurally closed and undisturbed, laterally continuous and free of small-scale discontinuities to store a large quantity of gas during a long period of time so the injected gas remains permanently confined. Illinois coal deposits tend to be thin, shallow and occur as multiple seams. One of the challenges associated with Illinois CO_2

sequestration projects is accurate and reliable mapping of the target coal seam(s). It has been suspected that since the conventional seismic waves have wavelengths larger than the thickness of the coal bed, the seams may be transparent to conventional seismic frequencies. This study focused on proving or disproving the applicability of advanced seismic techniques for producing reliable maps of thin Illinois coal seams for selecting the sites for CO_2 sequestration.

The next set of issues for CO_2 sequestration includes monitoring, verification and control. Ideally, a technique should be able to monitor the position of the injected gas in real time. Time-lapse seismic imagery (4-D seismic) appears to be the most promising remote sensing technique available for monitoring, verification and control of processes on the scale of CO_2 sequestration projects. This technique has been successfully used for more than a decade to monitor the movements of gas injection in conventional oil and gas reservoirs. The principle behind the technique is reduction in seismic velocity and bulk modulus resulting from the advance of a gas phase into the liquid saturated body of porous rocks. The challenge associated with using this technique in coal beds is that coal in itself is quite compressible relative to conventional sedimentary rocks and has relatively low acoustic velocity and elastic moduli. The goal was to determine whether seismic velocity changes caused by addition of a gas phase into the coal cleat system would be large enough to be resolved by seismic imaging. The laboratory work performed in this project was designed to test this issue.

Imaging the expansion of the gas front during CO_2 injection serves two auxiliary goals:

- to ensure the injected gases remain within the target zone, the flow direction must be defined and the position of the gas front must be projected for the life of the project. This requires knowledge of spatial permeability variations and determination of high permeability trends; and
- injection of CO_2 into coal seams containing adsorbed methane causes the release of methane that can be produced. To produce the methane evolved through CO_2 sequestration, the production wells must be placed along the preferred flow path. The direction and progress of the gas front is set by the direction of least resistance to flow (the high permeability trend).

It should be noted, however, that no reliable geophysical techniques for determining permeability of subsurface sediments are available. In the absence of any direct measurement tool, effects of lateral permeability variations may only be observable through time-lapse seismic surveys. In these surveys, progress of the gas front is mapped after preset time periods; the duration of which is determined from reservoir engineering studies. Integrating the seismic information with reservoir data within the local geologic framework could provide a dependable tool for predicting the flow direction, which can then be used to select locations for injection and production wells as well as planning for remedial actions if necessary.

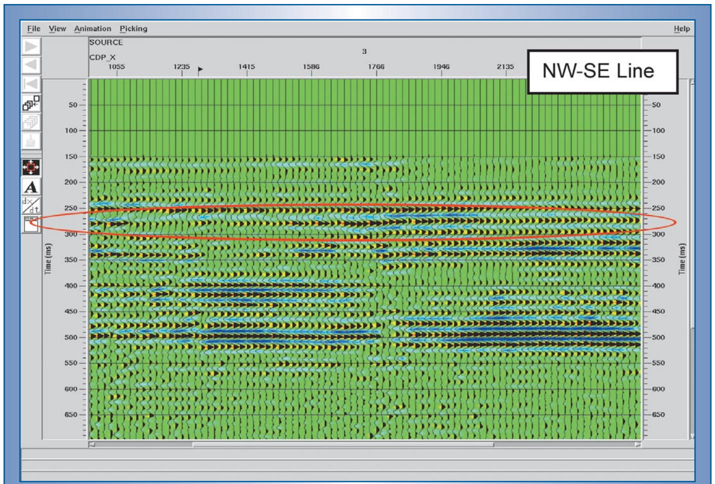

Figure 2. Processed seismic section for line 1,000.

Field experiments

Although the resolution of seismic techniques for conventional sedimentary rocks is rarely better than 16.4ft, Van Reil (1986) has shown coal beds as thin as 2.46ft can be resolved by reflection seismic methods. The higher resolving power of seismic techniques for coal seams is because of the high reflection coefficient at the interface between the coal and contiguous sand or shale beds. It has been established that for a normal incident wave the amplitude of incident and reflected waves follow this relationship:

$$A_2/A_1= (\rho_2V_2 - \rho_1V_1)/(\rho_2V_2 + \rho_1V_1)$$

Where A_1 and A_2 are the amplitudes of incident and reflected waves, ρ_1 and ρ_2 are the densities of the interfacing beds and V_1 and V_2 are the corresponding seismic velocities. In the case of coal seams, the impedance contrast between the coal seam and the interfacing beds is exceptionally high because the density and velocity values for coal are much smaller than those for the interfacing shale or sand beds. For example, when a coal seam with 1.2 g per cu cm density and 3,937.2ft per second seismic velocity interfaces with a sand bed with 2.2 g/cc density and 8,205.5ft per second velocity, the reflection coefficient will be 0.585, meaning nearly 58% of the energy will be reflected from the interface.

Widess (Widess et. al., 1986) showed the amplitude of a seismic wave reflected from a thin bed or seam can be calculated by $4\pi\alpha\beta/\lambda$, where α is the reflection amplitude of the bed (assuming a thick bed), β is the bed thickness, and λ is the wavelength. Seismic resolution is thus proportional to the reflection amplitude, bed thickness and wavelength. Widess concluded the thickness of a bed must be at least one-eighth of the dominant seismic wavelength to be resolvable. Thus, a key question to be addressed was whether advanced seismic techniques could identify individual coal seams within a coal “package” or whether the overall low frequency signal from the package would mask the individual high frequency event(s).

Table 1. Coal seams encountered in well Hon No. 9.

Coal	Top (ft)	Base (ft)	Log Thickness (ft)	Core Coal Thickness (ft)
Danville	*758*	*762*	*4*	*3.6*
Herrin No. 6	*806*	*810*	*4*	*5*
Springfield No. 5	*882*	*886*	*4*	*4*
Houchin Creek No. 4	*971*	*972*	*1*	*1.5*
Survant No. 3	*996*	*1,000*	*4*	*4.1*
Colchester No. 2	*1,066*	*1,068*	*2*	*1.6*
Davis—upper split	*1,110*	*1,111*	*1*	*1.4*
Davis—middle split	*1,114*	*-*	*-*	*2.1*
Davis—lower split	*-*	*1,118*	*4*	*1.2*

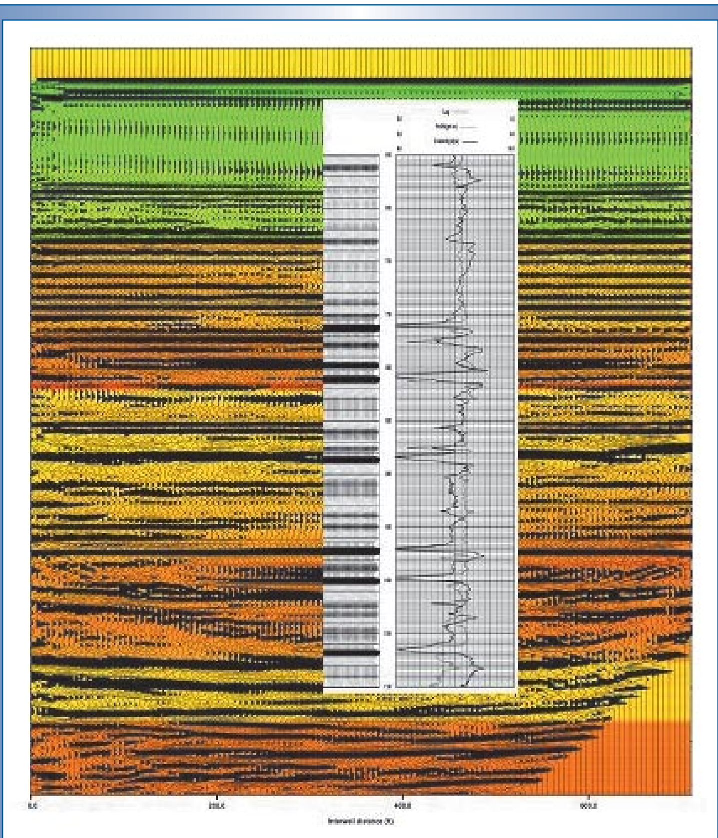

Figure 3. Final cross-well image.

To answer this question, a series of seismic data acquisitions were carried out in White County, Ill., at the Illinois State Geological Survey (ISGS) pilot site (Figure 1). These were four densely-populated surface lines plus one vertical seismic profile (VSP) and one cross-well survey.

The frequency content of surface seismic data is usually less than those of VSP and cross-well data because the earth materials between the seismic source and receiver act as a high-cut filter eliminating the higher frequency content of the seismic events. In VSP, where the receivers are lowered inside the wellbore and the source is on the surface, the shot receiver distance is almost halved, thereby preserving more of the high frequency content. In cross-well systems, where the seismic source and receiver are placed inside the wellbore, the highest frequencies are maintained leading to the highest possible resolution. The multiple survey approach allowed us to use a wide seismic frequency range to evaluate the merits and limitations of each seismic technique relative to the common coal conditions in Illinois.

ISGS drilled and cored a well (**Hon No. 9**) in the center of the pilot site and made this well available for VSP and cross-well surveys. Nine coal seams, each between 1.2ft and 5ft in thickness were cored at this site (Table 1).

Information from this well was used in our survey design to assure the field efforts would lead to useful data and knowledge. These seams were thinner than anticipated and created a challenge to seismic resolution.

The goal of the field study was to determine which acquisition geometry (or combination of geometries) was best suited for imaging the coal seam continuity. Cross-well data (frequencies of more than 500 Hz) was expected to have the highest resolution but required the presence of two wells spaced less than 700ft apart for deployment of sources and receivers and only provided a 2-D slice of the inter-well region. VSP was expected to have resolution intermediate between cross-well and surface seismic. 3-D images can be obtained from VSP data, but the coverage is limited to a ring about half of the target depth (in this case, about 500ft from the receiver well), and surface seismic provides the largest area coverage but has the lowest resolution.

The design was completed and then implemented in December 2003. To optimize the resolution of the surface seismic and VSP, a high frequency IVI-2 MiniVibe capable of sweeping up to 500 Hz was used in this study.

To optimize resolution, 40-Hz geophones were used to record the surface seismic data. Ninety-six surface receivers were spaced at 18-ft intervals to ensure high frequency data would not be spatially aliased. Line 1,000 (shown in figures 1 and 2) is the line running across the two wells used for the cross-well survey and is the northwest to southeast line shown in Figure 1. Lines 2,000, 3,000 and 4,000 were run perpendicular to line 1,000 for the purposes of understanding out-of-plane heterogeneity in line 1,000 and in the cross-well data. For each line, the receivers were fixed, and the vibration points were located every 36ft from the end of the receiver "spread" in each direction for 1,500ft. This survey geometry resulted in a full fold extent of about 0.3 miles per line. For each source point, four 7-second linear sweeps (20 Hz to 400 Hz, 1 second listen) were correlated and stacked. The data was recorded using the distributed Geometrics Geode system. The data was digitally sampled at 0.5-millisecond intervals using a 24-bit sigma-delta converter and written to SEG-D format.

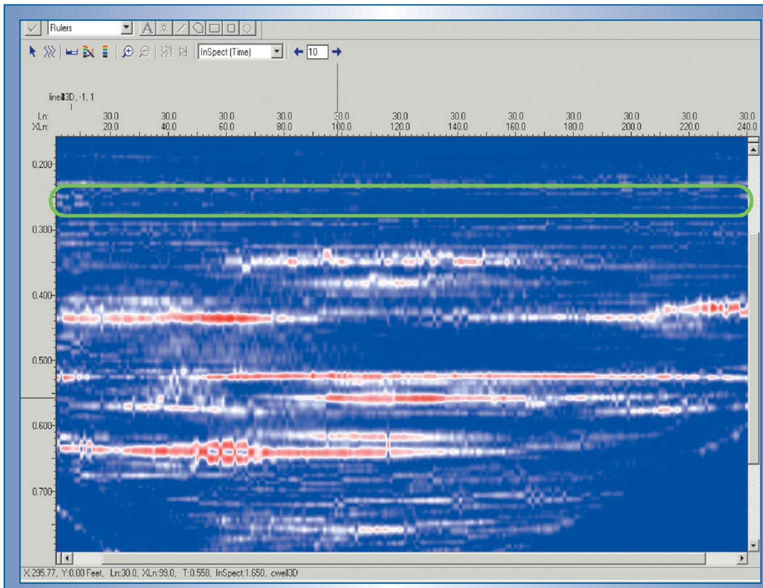

Figure 4. Spectrally decomposed data at 30 Hz.

In December 2003, Z-Seis Corp., under contract with Gas Technology Institute (GTI), acquired one cross-well seismic survey between the Hon 9 and **Hon 3** wells. During the initial cross-well logging, it was discovered that the Hon 3 well could only be logged to the depth of 830ft instead of 1,018ft because of the plug slipping up-hole during cementing. The survey was logged with this depth restriction. Externally generated surface noise during logging required re-logging of the site. Hon 3 was deepened to 985ft and the survey re-acquired by Z-Seis as their in-kind contribution to the Illinois Clean Coal Institute/GTI project.

Field data acquisition results

Seismic data acquisition included the recording of four densely-instrumented lines, VSP and a cross-well survey. The major finding from the field data acquisition task was that, under the ISGS site conditions, conventional seismic recording provided images of the coal package but fell short of identification of individual coal seams. This was mainly because of the overburden (Tick river fill) at the site and the incompetent nature of the overburden causing severe attenuation of the high frequency content of the seismic waves. In contrast, cross-well signals and VSP data, to a lesser extent, were rich in high frequencies. It is therefore recommended that under similar conditions, cross-well seismic surveys should be used to provide the most reliable images of the subsurface. These images also can be used for identification of refection horizons on surface sections. Although VSP data is more reliable than surface data, the signals are still subject to surface related attenuation.

Because of poor surface coupling, Vibroseis should not be the source of choice for seismic surveys. Instead, impulsive sources, such as small explosive charges, placed about 10ft below the surface would be preferred. In addition to starting with a wide band of energy at the source, coupling of the source energy to the ground would be enhanced.

Data analyses included all conventional seismic analysis techniques to produce the final cross sections. The success of the project was keyed to development of accurate cross sections by integrating the results from all

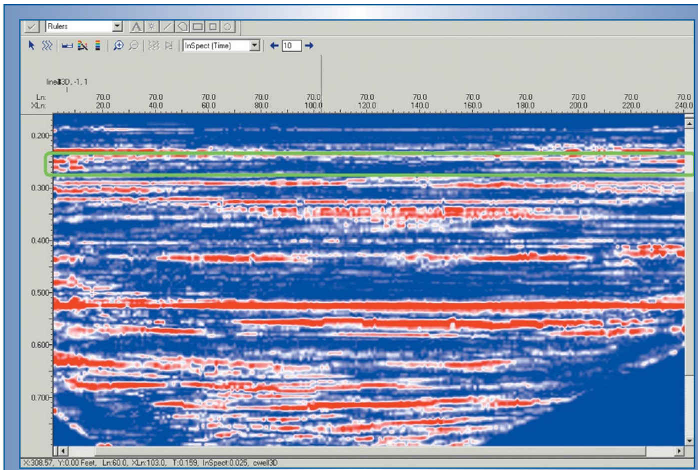

Figure 5. Spectrally decomposed data at 70 Hz.

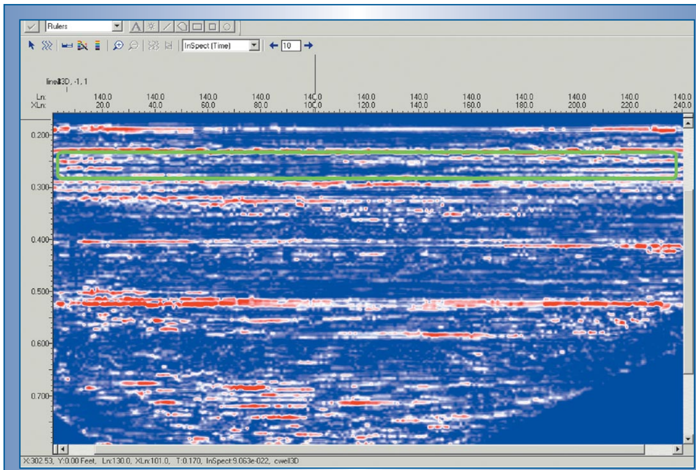

Figure 6. Spectrally decomposed data at 140 Hz.

three surveys. Figure 2 is the final processed seismic sections from surface lines shown on Figure 1. Note that although the reflection events from the coal package (inside the red ellipse) are clearly identifiable, individual coal seams have been transparent. Also note that the coal package as a whole is continuous and does not exhibit any discontinuity. Lower in the section, at about 400 milliseconds, discontinuity is observed. These discontinuities do not appear to reach the coal zone and do not cause concern.

Figure 3 is the final processed cross-well image, which covers the section between wells Hon 3 and Hon 9. All coal seams present at the site have been imaged, as shown by the superposition of the well log and core data.

To identify the dominant frequency for coal seams and determine changes in frequency with depth, the data was spectrally decomposed in 10-Hz increments for the entire section. Figures 4 through 6 are example frames of results from these analyses. Note that at 30 Hz (Figure 4), the resolution at the zone of interest is low; it is noticeably enhanced at 70 Hz (Figure 5) and is at the highest value at 140 Hz (Figure 6).

Following completion of the data analysis and visualization, a series of seismic forward modeling was performed. The purpose of the modeling was to investigate the feasibility of time-lapse seismic technology for imaging the injected or evolved gas phase within the coal seams. Results from laboratory measurements showed that addition of a gas phase to initially water-saturated coals would cause substantial decrease in the compressional wave velocity. However, in our modeling, a conservative 20% velocity reduction was assumed. Results from these modeling efforts are shown on Figure 7 where the line graphs on either side of the colored area represent the well logs from wells Hon 3 and Hon 9. Coal seams can be identified on these logs. Each vertical band on the main figure was for a range of frequencies that increases to the right, such as low frequency band on the left (10 Hz to 50 Hz) and high frequency band (100 Hz to 1,200 Hz) on the right. The top part of the figure exhibits the seismic response of individual seams before velocity reduction and the bottom part shows the response after 20% velocity reduction. Note that changes in the seismic response resulting from injection of CO_2 or evolution of coalbed methane can only be observed at frequencies in the 100-Hz to 800-Hz and 100-Hz to 1,200-Hz bandwidths (area within the blue rectangles). Results from forward modeling work suggest that accurate monitoring of the injected CO_2 front through repeated cross-well surveys is possible.

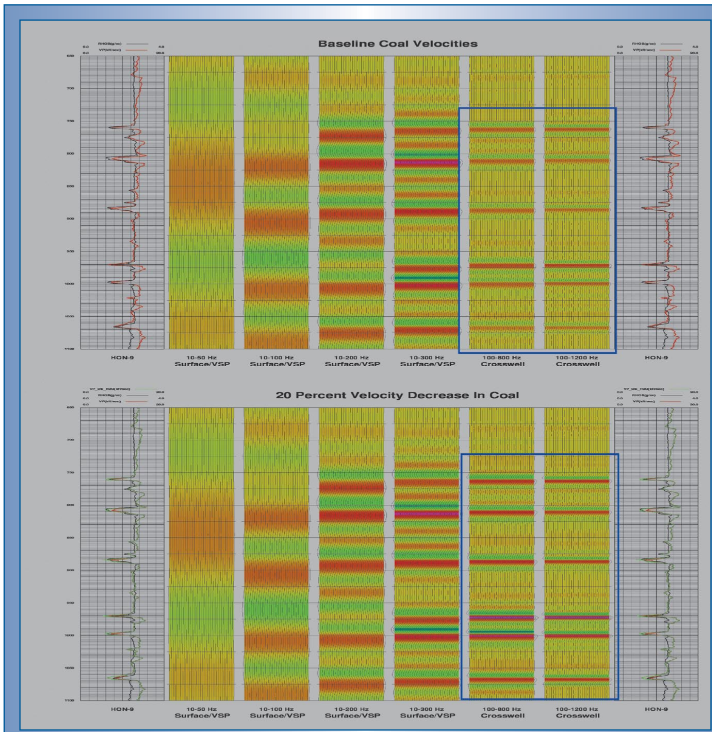

Figure 7. Response of individual coal seams to gas saturation.

Conclusions and recommendations

Combining the results from the actual surveys, spectral decomposition and forward modeling, the following conclusions can be drawn:

- at 10 Hz to 50 Hz bandwidth, the resolution is low and results from surface seismic surveys are not reliable;
- at 10 Hz to 200 Hz bandwidth, high resolution imaging is possible, and surface seismic data would be reliable for mapping of the "coal seam packages" as a whole;
- the use of impulsive sources for surface seismic surveys is strongly recommended;
- VSP surveys (10 Hz to 300 Hz bandwidth) noticeably enhance the resolution; and
- under geologic conditions similar to those at the ISGS pilot site, position of the injected or evolved gas can only be imaged at higher frequencies through cross-well seismic applications. ✧

Acknowledgements

The authors wish to express their acknowledgments to the Illinois Clean Coal Institute and Gas Technology Institute for their financial support, and to Dr. David Mores of the Illinois State Geological Survey for their technical support and contributions. Thanks also to Mr. Jim Cantrell of Royal Drilling Co. for his valuable logistical and operational support and to Z-Seis for their coordination of the field work and contribution of a second cross-well survey at no charge.

References

1. Van Riel, W. 1986. Coal Geophysics, *Society of Exploration Geophysicists.*

2. Telford W.M., Geldart L.P., Sheriff R.E, and Keys D.A. Applied Geophysics, *p 251-252, Cambridge University Press, 1978.*

3, Widess et. al. 1986. Coal Geophysics, *Society of Exploration Geophysicists.*

Selecting Strategies for Improving Fracture Performance in Tight Gas Sands

By Mukul M Sharma, Phani Gadde, Y. Liu and J. Mahadevan, *University of Texas at Austin*; and Richard Sullivan, *Anadarko Petroleum Corp.*

A U.S. Department of Energy-sponsored project at the University of Texas at Austin and Anadarko Petroleum Corp. conducted during the past 2 years has focused on strategies for improving productivity in the Bossier play in East Texas. Some lessons learned from the six-well field study have been applied to wells in other tight gas sand assets.

This article summarizes some of the strategies used to improve fracture performance. The key to the successful application of these strategies is the selection of a specific strategy and fracture design for a specific well based on an analysis of its data. The development of 3-D hydraulic fracture models capable of accurately modeling proppant transport and fracture propagation is crucial to the successful selection of these strategies in tight gas formations over a broad cross-section of tight gas sand assets with varying stress regimes and formation properties.

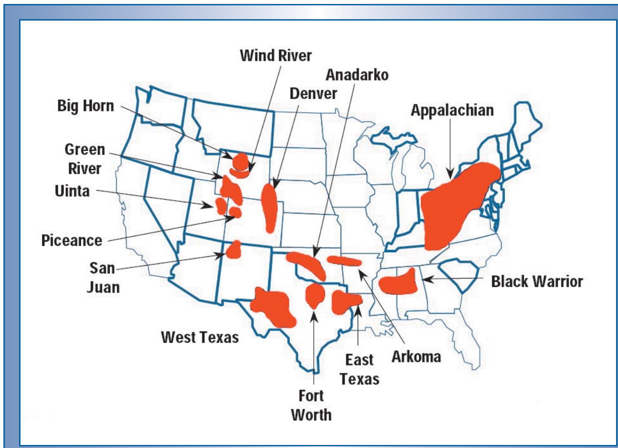

Figure 1. Resource base for tight gas sands in the United States. (Source: United States Geological Survey)

The tight gas resource base

Figure 1 shows the resource base for tight gas sands in the United States. Estimates place the gas reserves in tight gas sands at 59 Tcf, which constitutes about a third of the total domestic gas reserves of 189 Tcf. Tight gas sand assets have a wide geographic spread and vary in depositional environments, subsurface stress regimes and reservoir properties. Consequently, fracture designs successful in one field frequently are unsuccessful in another. Developing a successful fracture design strategy for a field should be based on field experience guided by data-calibrated fracture models.

DOE-UT-Anadarko Dowdy Ranch test wells

Six test wells and two data wells were selected (**APC Anderson No. 1** and APC Anderson **No. 2**) for conducting extensive analysis of petrophysical and other data to evaluate fracturing strategies. Some results from the micro-seismic monitoring, well logs, core data and production response are discussed in reference 1.

Analysis of the production response from a large number of fracs in the Bossier sands indicates that traditional gel-fracs often perform poorly (and are more expensive) compared with slick-water fracs. A likely cause of the poor performance of the gel-fracs is gel-plugging of the proppant pack, which has lead to the widespread use of slick-water fracs and variations of it (hybrid fracs). Slick-water fracture treatments designed for frac lengths between 600ft and 800ft yield effective fracture lengths (obtained from production response and/or pressure buildup analysis) that are seldom more than between 80ft and 150ft. This difference in propped fracture lengths and created fracture lengths has been documented in reference 2. It has been postulated that the small effective fracture lengths obtained primarily are the result of proppant settling in low-viscosity fluids, which has led to the application of hybrid fractures in some wells. Micro-seismic data collected from the Dowdy Ranch test wells indicate created fracture lengths between 600ft and 700ft, and effective fracture half lengths between 150ft and 250ft for hybrid fracture treatments. Using a smaller 40- to 70-mesh proppant, instead of 20 to 40 mesh, also has resulted in significant improvements to well productivity in most cases. However, in some fields, the application of hybrid fractures or the use of smaller proppant does not yield any significant benefits and may cause a reduction in the productivity of the wells. No clear guidelines are available for an operator to indicate when a hybrid fracture would be warranted as opposed to a slick-water treatment, a gel frac or whether other treatment designs should be considered. To develop better selection criteria for fracture designs, lab data and models for proppant

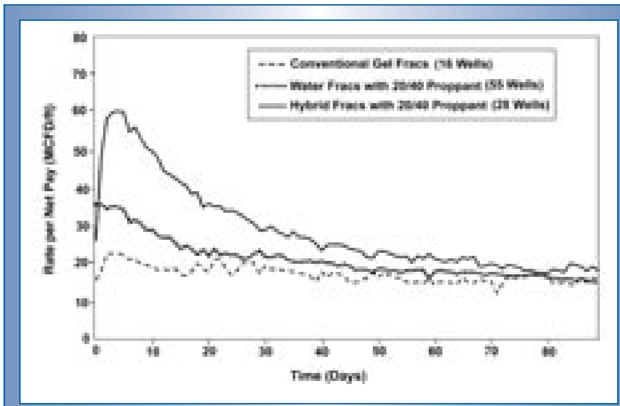

Figure 2. Hybrid fracs outperform slick water and gel fracs in Bossier sands.

placement in slick-water, hybrid-fracs and other more complex fracture designs were developed as part of this U.S. Department of Energy (DOE)-sponsored study.

Laboratory and modeling studies

An experimental study was undertaken to investigate the impact of fracture width and fluid rheology on proppant transport, including particle settling and horizontal transport. Experiments were conducted in a fracture flow cell for Newtonian fluids as well as shear thinning fluids with varying viscosities. New models for proppant transport and settling in hydraulic fractures were developed and implemented in a 3-D hydraulic fracturing code. The proppant-settling models developed account for changes in the settling velocities and rheology caused by fracture walls, proppant concentration, turbulence effects because of high fluid velocities and inertial effects associated with large relative velocities between the proppant and the fluid. Proppant velocity relative to the fluid in the direction of flow is affected by the fracture walls and can result in significant reduction in the proppant transport. A model was developed to estimate the proppant retardation (ratio of particle velocity to the fluid velocity) because of these effects. These correlations have been incorporated into a fully 3-D hydraulic fracture code, UTFRAC-3D.

In addition to proppant settling, using slick-water fracs also raises concerns about the loss of large volumes of water-based fluids into low permeability, low-water saturation sands. The loss of water-based fluid results in significant water-blocking problems and can retard the flow of gas back into the well. Using slick-water fracs in some situations may, therefore, not be the optimum fracture treatment. Gel-induced damage of the proppant pack vs. water blocking of the tight gas matrix is a choice that may need to be made.

The following sections contain examples of some fracturing strategies used in the past with varied success. However, the selection of a particular strategy for a particular field and its optimization during time has been based largely on field experience – a trial and error basis. By conducting hydraulic fracture simulations that incorporate realistic models for proppant transport and fracture propagation, the selection of an optimal fracturing strategy can be sped up and performance predictions made with a greater degree of confidence.

Strategy 1—Hybrid fracture treatments

The placement of proppant can be significantly improved by using cross-linked gels during the proppant pumping stage. These treatments are referred to as hybrid-fracs and provide two key benefits:

- minimize the settling of the proppant, resulting in deeper placement of the proppant pack; and
- larger fracture widths allowing the proppant to flow more easily into the fracture and avoiding proppant bridging problems.

However, two important facts need to be kept in mind when using hybrid-fracture treatments. The proppant pack in hybrid fractures is still susceptible to gel damage since the gel carries the proppant. Secondly, since the net pressure required to inject cross-linked gel may be significantly higher than for slick-water fracs, significant vertical growth of the fractures may be expected. Insufficient stress contrasts in many situations may result in undesirable vertical growth of fractures, resulting in shorter propped fracture lengths and sub-optimal well performance.

A comparison of hybrid-fractures with slick-water fracs and conventional gel fracs is provided in Figure 2. In the Bossier trend, hybrid-fracture treatments work significantly better than slick-water fracs in terms of well productivity. Counter examples to this can be found in the **Carthage** field where slick-water fracs have performed just as well. Hybrid fracs should, therefore, be applied only when gel-induced damage and vertical fracture height growth concerns can be adequately addressed. Checking for fracture containment using mini-frac tests and 3-D fracture simulations at different injection rates, rheologies and proppant loadings can prove a valuable tool for selecting between slick-water and hybrid fracs as well as designing an optimal fracture treatment.

Strategy 2—Optimizing fluid rheology and rates

Using uncross-linked fluids with lower polymer concentrations provide an opportunity to reduce the net pressure required to propagate the fracture and place the proppant. When the stress contrast between the sand and the shales is small, it may be desirable to pump fracture treatments with uncrossed-linked fluid so vertical height growth can be minimized. This strategy requires detailed modeling of proppant flow into the fracture since smaller net pressure also will result in smaller fracture widths, which may lead to proppant bridging and tip screen out. Figure 3 shows an example of the optimum fluid rheology needed to propagate a fracture with a stress contract of 200psi between the sand and the shale. Using relatively low viscosity fluids

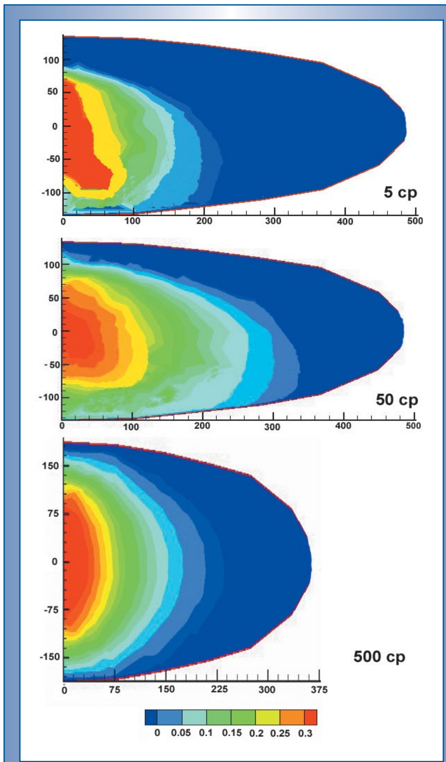

Figure 3. Selection of the proper fluid rheology is crucial for obtaining long propped fracture half-lengths (red, yellow and green). Viscosity that is too low or high will yield short propped fractures. Note that created fracture half-lengths (blue) are less sensitive to fluid rheology.

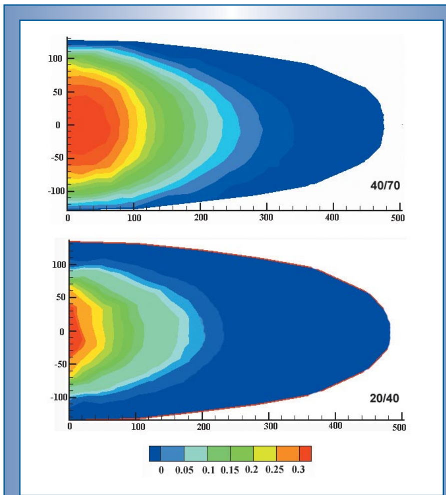

Figure 4. Effect of proppant size on proppant placement.

(10 cp to 100 cp at shear rates in the fracture) can reduce the settling rate of the proppant to an acceptably slow rate while allowing the net pressure to be small enough for the fracture to remain contained. The specific rheology and rates used can vary depending on the proppant size used, the *in-situ* stress contrast and other mechanical properties of the sands and shales. An answer to the optimum fluid rheology cannot be provided apriori without adequate stress and leakoff data and a fracture simulator that accurately models proppant transport as well as fracture containment.

Strategy 3—Small or lightweight proppant

Using smaller proppant sizes (between 40 and 70 mesh as opposed to 20 and 40 mesh) has improved the performance of slick-water fracs in the Bossier. Recent work with lightweight proppants also shows productivity improvements at depths where proppant crushing is small. In both cases, the rate of proppant settling in the fracture is significantly reduced. Recent work conducted at the University of Texas shows the transport of proppant is affected by the ratio of the proppant size of the fracture width. As the proppant size approaches the fracture width, the flow of the proppant is significantly retarded, particularly for cross-linked fluids, resulting in short propped fracture lengths. The significance of proppant size on proppant placement is only evident if proppant transport, settling, retardation, bridging and TSO effects are properly accounted for. Figure 4 shows an example of the impact of proppant size on propped fracture half-lengths.

Strategy 4 —Minimizing impact of water blocking in depleted sands

The removal of water blocks in tight gas sands occurs in two stages. The first stage is the displacement of water that occurs during a short time period (about 100 pore volumes). Following this short duration recovery of frac fluid (usually only a small percentage of the fluid is recovered), the long-term clean up of the gas well occurs primarily by water vaporization because of the flowing gas, which becomes under-saturated as its pressure decreases. Vaporization effects have not been considered in earlier studies of water-block clean up and have a profound effect on the productivity index of low permeability gas wells.

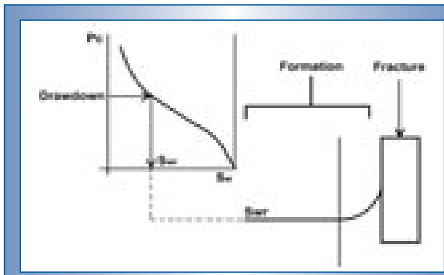

Figure 5. Residual water saturation that will be left behind at the end of displacement. This water is removed by evaporation during several weeks of gas production.

The extent of water blocking achieved in a given situation depends on the drawdown available as well as the capillary pressure curve for the rock. Figure 5 shows the remaining water saturation left behind at the end of displacement. The higher the drawdown, the lower the water saturation and the higher the well productivity. However, the productivity of gas wells improves during long periods of time. Lab experiments conducted in this research show that this is primarily because of water vaporization due to the reduction in gas pressure as it flows into the fracture.

Using slick-water fracs should be limited to wells in which the ratio of drawdown available to the capillary pressure at a water saturation of 50% is greater than 1. This ensures that the water saturation around the fracture can be reduced to below 50% during the displacement stage of flowback. Such a condition may not be met in re-fracturing situations or when fracturing infill wells where the reservoir pressure has been significantly depleted. In such situations, water-fracs should be applied with caution. Reservoir temperature has a significant effect on clean up. Higher temperature wells will cleanup more easily than lower temperature gas wells. Using surfactants may be an option in some highly-depleted, low-permeability sands.

Strategy 5—Multistage fracture treatments

In the work conducted in the Bossier, bullheading fracture treatments into multiple zones result in well productivities significantly lower than staged fracture treatments. Figure 6 shows an example of a single-stage vs. a multi-stage fracture treatment conducted in two adjacent wells (APC No. 1 and APC No. 2). The gas production per net foot of pay is significantly higher for the multistage treatments. This observation has been consistently made in other wells and by other operators.

Strategy 6—Reverse hybrid fracs

In hybrid fracs, the creation of the fracture with slick water is followed by proppant placement using a cross-linked gel. In reverse hybrid fracs, a term coined in this article, the fractures are created using a polymer gel pad while the proppant placement is conducted using slick water.

This strategy for placing the proppant has two significant advantages:

- the cross-linked fluid pad results in larger fracture widths allowing easier placement of the proppant; and
- the slick water carrying the proppant has a lower viscosity than the cross-linked gel. This results in viscous fingering of the proppant slurry into the gel. The proppant is, therefore, placed in viscous fingers, non-uniformly across the fracture height resulting in deeper placement of the proppant into the fracture in many cases.

This strategy allows proppant to be placed deep into the fracture, even though the entire fracture height may not be propped. A sample lab result (Figure 7) shows how the layers of gel prevent settling of the proppant to the bottom of the fracture. Field experience shows that under certain conditions, reverse hybrid fracs are more effective than hybrid fracs in creating longer effective frac lengths. A lot more needs to be done to understand and model these reverse hybrid fracs in more detail so candidate well selection for these types of treatments can be made in a more systematic manner.

Summary

Laboratory and modeling work conducted at University of Texas as well as field experience in Anadarko wells in the Bossier have resulted in improvements to the understating of proppant placement in tight gas sands. The selection and application of any of the strategies discussed above should be guided by modeling of the process of fracture creation and proppant placement using fully 3-D fracture models. Without such studies, many of these strategies, which are effective in some locations, may prove ineffective in others. ✧

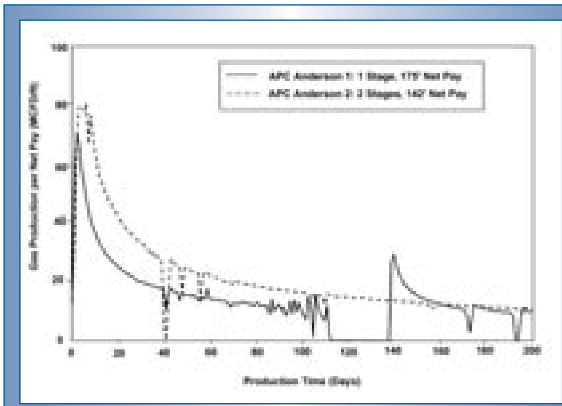

Figure 6. Comparison of gas production per foot of pay for single- vs. multi-stage fracture treatments.

Figure 7. A slot-flow experiment showing proppant distribution in a reverse hybrid fracture treatment. The layers of gel created because of viscous fingering prevent settling of the proppant to the bottom of the fracture.

References

1. *Sharma, M. M.., P. B. Gadde, R. Sullivan, R. Sigal, R. Fielder, D. Copeland, L. Griffin and L. Weijers,* Slick Water and Hybrid Fracturing Treatments: Some Lessons Learnt, *Journal of Petroleum Technology, March 2005.*

2. *Rushing, J.A. and R. B. Sullivan,* Evaluation of Hybrid Water-Frac Stimulation Technology in the Bossier Tight Gas Sand Play, *SPE Paper No. 84394, presented at the SPE Annual Technical Conference, Denver, October 2003.*

3. *Liu, Y. and M. M. Sharma,* Effect of Fracture Width and Fluid Rheology on Proppant Settling and Retardation: An Experimental Study, *SPE Paper No. 96208 to be presented at the SPE Annual Technical Conference and Exhibition, Dallas, Oct. 10-12, 2005.*

4. *Gadde, P. B., Y. Liu, J. Norman, R. Bonnecaze, and M. M. Sharma,* Modeling Proppant Settling in Water-Fracs, *SPE Paper No. 89875 presented at the SPE Annual Technical Conference and Exhibition, Houston, Sept. 26-29, 2004.*

5. *Gadde, P. B. and M. M. Sharma,* The Impact of Proppant Retardation on Propped Fracture Lengths, *SPE Paper No. 97106, to be presented at the SPE Annual Technical Conference and Exhibition, Dallas, Oct. 10-12, 2005.*

6. *Mahadevan, J. and M. M. Sharma,* Clean-up of Water Blocks in Low Permeability Formations, *SPE Journal, September 2005.*

7. *Mahadevan, J., M. M. Sharma and Y.C. Yortsos,* Evaporative Clean-up of Water-Blocks in Gas Wells, *SPE Paper No. 94215, presented at the SPE Production Operations Symposium, April 2005.*

Real-time Pore-pressure Prediction Ahead of the Bit*

Cengiz Esmersoy,
Schlumberger and
Subhashis Mallick,
WesternGeco

High formation pressure continue to be one of the major problems for the drilling industry, especially in deep waters. Integrated processing of seismic data and real-time logging-while-drilling measurements can provide a significantly improved pore-pressure estimate as the well is being drilled.

In this article, the prediction capability of seismic data is combined with the actual measurements of the real-time logs in predicting an elastic model. A new logging-while-drilling (LWD) tool, called seismicVISION**, providing real-time checkshot measurements while the well is being drilled, makes such a combination possible. All available real-time logs including P- and S-wave sonic and density, calibrated by the seismicVISION check-shot data, are used to obtain the actual elastic model down to the depth of the drillbit. We then run prestack waveform inversion by constraining the initial model exactly to the measured model parameters above the drillbit, which allows an accurate prediction of the elastic earth parameters ahead of the bit. These parameters, in turn, can be used in predicting pore pressure of formations and the position of reflectors. Using real seismic data, we demonstrate such a methodology can be used to predict pore pressure ahead of the drillbit in real time.

Estimation of abnormally high formation pore pressure is important in deepwater seismic exploration. The pore pressure, together with fracture gradient, determines the amount of mud weight needed to maintain the wellbore stability. Too much mud weight fractures the rock and too little allows formation fluids to come into the well and cause blowouts.

In a review article, Dutta (2002) gives a detailed and comprehensive account of various pressure prediction methodologies available in the industry. Pore pressures prior to drilling are typically estimated from seismic velocities. These seismic velocities, obtained from a conventional velocity analysis of prestack seismic data, are mapped into the pore pressures using a velocity-pressure transform for a given region.

A second method of pore-pressure estimation is the real-time logs obtained as the well is being drilled. LWD sonic logs with geologic models were used in the Gulf of Mexico to predict pore pressure. In areas with normal pressure, a normal compaction of sedimentary rocks causes velocities to increase with depth. If the sonic log velocities show a consistent slowing trend away from the compaction curve predicted by the geological model, it is used as a likely indicator of increased pore pressure ahead of the bit.

These methods are successfully used in practice but have shortcomings. In the predrill pore-pressure estimate, the conventional velocity analysis can have large uncertainties depending on the area, acquisition geometry and target depth. This uncertainty often does not allow the pressures to be predicted with a great accuracy down to the reservoirs several thousands of feet deep. The LWD-based method has the advantage that the real-time measurements close to the region of interest

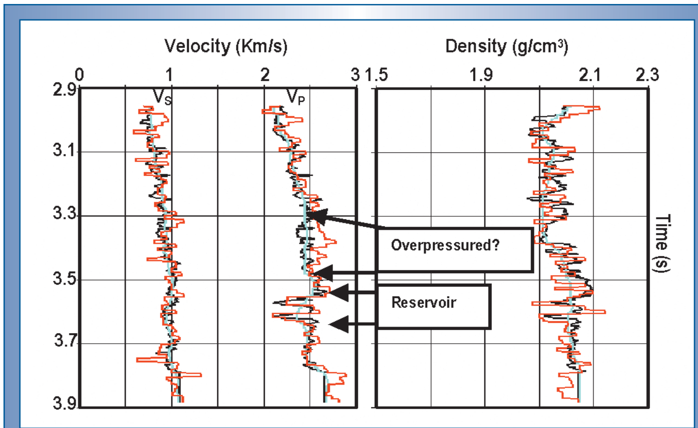

Figure 1. Prestack waveform inversion results using a standard workflow. The initial model is in cyan, the inverted model in red and the true model from the well data in black. The reservoir zone and a possible over-pressured formation above the reservoir are marked.

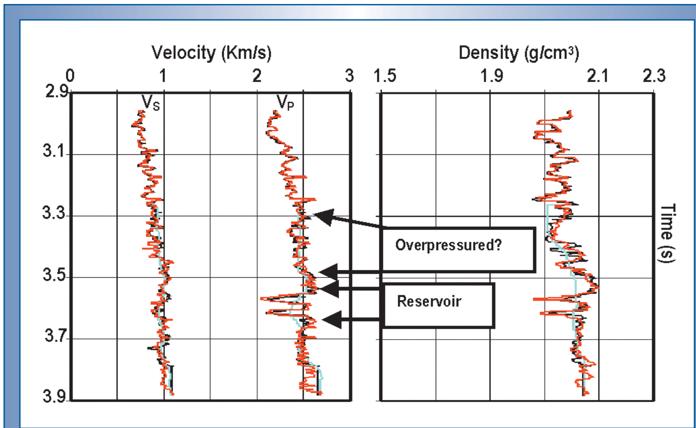

Figure 2. Prestack waveform inversion result when the model is constrained to the exact checkshot corrected well model down to 3.26 seconds two-way time. Notice this constrained inversion matches the well model to a greater accuracy than the one shown in Figure 1.

are used in predicting pore pressure. It is, however, not a true look-ahead technique as this method can be used to predict pressures to only a few hundred feet ahead of the drillbit. Consequently, neither surface seismic data nor LWD logs by themselves provide the best possible pore-pressure estimate ahead of the bit.

In this article, we combine the prediction capability of seismic data with the actual measurements of the real-time logs to accurately predict pore pressures to thousands of feet deeper than the bottom of the well. We use the new LWD tool called seismicVISION that provides real-time checkshot measurements while the well is being drilled. We also use all available real-time logs, such as P- and S-wave sonic and density, and calibrate them by the seismicVISION checkshot data. Such calibrated logs then provide an accurate description of the elastic earth model down to the bottom of the well. The entire prestack seismic data is then inverted using a nonlinear prestack waveform inversion (PSWI) methodology. In running PSWI, the initial earth model is constrained down to the bottom of the well to the exact model as obtained from the calibrated real-time logs. Such a constrained PSWI run obtains an accurate elastic earth model several thousands of feet deeper than the bottom of the well. This accurate model can then be used in real-time pressure prediction down to the reservoir depths.

Example

Figure 1 shows PSWI results of a real data set from the Gulf of Mexico using a standard PSWI workflow. The initial model is shown in cyan, the inverted model is shown in red, and the actual model from the checkshot corrected log measurements is shown in black. The reservoir zone is about 3.6 seconds as marked on the figure. Overall, the inversion results match the true model, especially at the reservoir level. However, there is a slowing trend of the V_P field, just below 3.3 seconds that is not resolved in the inversion. Such a slowing trend in the velocity field could be indicative of an over-pressured formation. Therefore, although PSWI gave a satisfactory match at the reservoir level, if we were to use this inverted model in predicting pore pressures, we would under estimate the pressure above the reservoir. Such an under estimation of pore pressure, in turn, may have serious implications in maintaining well-bore stability while drilling.

To demonstrate the model prediction ahead of the drillbit, it is assumed the well down to a depth equivalent to 3.26 seconds of two-way time has been drilled. We therefore modify the initial model of Figure 1 to the exact well model down to 3.26 seconds and run PSWI modifying the model only below 3.26 seconds. The results are shown in Figure 2. Notice this newly constrained PSWI run can now predict the low velocity over-pressured zone above the reservoir accurately.

Discussion and conclusion

In our example, we have simulated a real-time model prediction scenario by assuming the log and check-shot data down to a certain depth is known. We used this information to constrain the inversion that predicts the earth properties below this depth. We then compared the inversion results with the actual logs to evaluate how well we did.

The constrained PSWI has several advantages. First, the constrained inversion yields more accurate predictions than the unconstrained one. Second, the constraints reduce the number of forward synthetic computations needed in PSWI, leading to a rapid convergence of the algorithm. On a Linux cluster of 10 2 GHz Pentium 4 nodes, the inversion shown in Figure 2 took 15 minutes to run while the inversion shown in Figure 1 took about one hour.

Faster run time for constrained PSWI makes our methodology feasible in real time while the well is being drilled. Sonic and density log data, collected in real time, to the depth of the well and calibrated by the seismicVISION check-shot data can be transmitted directly to the seismic processing center. Prestack seismic data can then be inverted using the proposed methodology at the processing center, and the inverted elastic earth model ahead of the drillbit can be transmitted back to the drilling site. This inverted model can, in turn, be used in predicting the pore pressure ahead of the drillbit and in choosing the mud weights required for further drilling. As the well is being drilled deeper, check-shot corrected logs can again be transmitted to the processing center to predict a model further below. This process can be continued throughout the drilling of the well. Such a continuous prediction of the elastic earth model using successive constrained PSWI runs will always ensure accurate pore pressure prediction well ahead of the drillbit and maintain wellbore stability throughout the drilling cycle of the reservoir. In addition to the pore pressure, inverted earth models provide a high-resolution definition of the layers ahead of the bit, which can help drillers with well placement. ✧

Acknowledgements

We thank Schlumberger and WesternGeco for permission to present this work.

References

1. *Esmersoy, C., Hawthorn, A., Durrand, C., and Armstrong, P.,* Seismic MWD: Drilling in Time, on Time, it's about Time, *The Leading Edge, 24, 56-62, 2005.*

2. *Dutta, N.C.,* Geopressure Prediction using Seismic Data: Current Status and the Road Ahead, *Geophysics, 67, 2012-2041, 2002.*

3. *Mallick, S.,* Some Practical Aspects of Prestack Waveform Inversion using a Genetic Algorithm: an Example from the East Texas Woodbine Gas Sand, *Geophysics, 64, 326-336, 1999.*

** A similar article previously was published in EAGE 67th Conference & Exhibition, June 2005.*

*** Mark of Schlumberger.*

Reducing Deepwater Drilling Costs Part 2—Riser Dilution and Cost Comparisons

By John Rogers Smith, Darryl A. Bourgoyne, John Shelton and Anuj Gupta
Louisiana State University

A study of dual-gradient deepwater drilling systems relying on riser gas lift and riser dilution concluded that both concepts are feasible and warrant additional research. Editors Note: This is the second in a two-part series.

This article will focus on liquid dilution of fluids in the riser as an alternative means for achieving a dual-gradient system as well as the expected costs savings that would result from using riser gas lift or liquid dilution instead of conventional drilling methods. These two methods are referred to as dual-density because the fluid density in the riser is different than that in the well. This article supplements part one of the series, which described the rationale for dual-density drilling and the investigation of riser gas lift as one mechanism for achieving a dual-gradient system.

Liquid dilution of riser mud

Liquid dilution of the drilling fluid in the riser is a potential alternative means of achieving a dual-gradient system. Two concerns regarding its feasibility were studied: the ability of the riser fluid used in a dual-density drilling system to retain sufficient solids suspension, and cutting transport properties after heavy dilution of the well fluid with an unweighted liquid are of critical importance. A practical system also requires that the mixed fluid that returns to the surface in the riser be separated into low-density and high-density streams for reuse.

This article supplements part one of the series, which described the rationale for dual-density drilling and the investigation of riser gas lift as one mechanism for achieving a dual-gradient system.

The investigation of the liquid dilution alternative began by studying potential drilling fluid formulations. The properties and formulations for practical deepwater drilling fluids were determined based on input from three major drilling fluid companies. The maximum drilling fluid density required for applying the dual-density concept to any of the actual deepwater wells studied was determined to be 17 lb/gal. Consequently, a number of lab samples of 17 lb/gal synthetic-based muds and a 7.6 lb/gal-dilution fluid with similar fluid makeup, but no weighting material, were formulated and evaluated for suitable properties individually and when combined to form a riser fluid. These lab formulations provided good emulsion stability and ideal densities, but it was not possible to achieve appropriate rheologies in both the weighted fluid and the riser fluid. Earlier tests reported by de Boer (2003), however, gave more favorable properties when using a lower density weighted fluid. It was concluded there was potential for favorable properties to be achieved, and evaluation of separation methods was deemed necessary. Separation experiments were conducted with a laboratory centrifuge and a 2-in. hydrocyclone from a "clay ejector" system used in processing mud in the field.

The centrifuge was able to separate the riser mud into near ideal densities for dilution and drilling fluid. However, the dense slurry retained in the centrifuge had lower emulsion stability than the feed stream. Separation using the 2-in. hydrocyclone achieved less contrast in density between the low- and high-density discharges, but consistently resulted in a beneficial increase in the stability of the mud emulsion and had more desirable rheological properties. Considering these results along with those for a field-scale centrifuge reported by de Boer, it was concluded that separation of riser mud into fluid streams suitable for use as a dilution fluid and a drilling fluid is feasible and should be practical for field application. The results of both Louisiana State University's tests and de Boer's test are shown in Table 1. Subsequent recirculation tests on fluids from the 2-in. hydrocyclone indicated a density contrast between the low- and high-density streams similar to that reported by de Boer can potentially be achieved using hydrocyclones in lieu of centrifuges. Future work is continuing to define an appropriate process flow design. Such work could result in an alternative to centrifuge separation with lower capital and operational costs and better resultant fluid properties.

The experiments also provided insight into meeting the challenge encountered in the tests on laboratory muds when trying to simultaneously meet the rheology requirements for the riser and wellbore mud streams. Separation with the hydrocyclone and de Boer centrifuge deliver fluids that come close to meeting these requirements. Apparently, the separation overflows contain fine residual barite particles and have a finer emulsion than the feed mud. These factors may be the key to achieving the desired viscosity for the riser mud without excessive viscosity in the wellbore mud. Comprehensive testing of a more complete hydrocyclone-based system and field-scale centrifuges is necessary to confirm this preliminary conclusion.

Table 1. Comparison of drilling fluid properties for pilot liquid-dilution dual density.

Mud Property	Louisiana State University Hydrocyclone			de Boer Centrifuge		
Mud Purpose	*Dilution*	*Riser*	*Wellbore*	*Dilution*	*Riser*	*Wellbore*
Density, lb/gal	*8.5*	*9.5*	*11.5*	*8.3*	*9.3*	*14.5*
PV, cp	*13*	*15*	*20*	*20*	*32*	*45*
YP, lb/100 sq ft	*11*	*14*	*15*	*7*	*12*	*20*

Table 2. Single-density well design for 17,000-ft total depth (6,000-ft water depth).

Hole Selection Interval	Depth Below Mudline	Bit Size	Mud Density	Kick Margin	Trip Margin	Casing Outer Diameter	Casing Setting Depth
ft-TVD-RKB	*ft-TVD-RML*	*in.*	*ppg*	*psi*	*psi*	*in.*	*ft-TVD-RKB*
6,000 (mudline)	*0*	*-*	*8.6*	*-*	*-*	*36*	*6,200*
6,000-8,000	*2,000*	*26*	*8.6*	*0*	*0*	*20*	*8,000*
8,000-8,900	*2,890*	*17½*	*9.5*	*200*	*125*	*16*	*8,890*
8,890-10,250	*4,250*	*14¾*	*10.4*	*200*	*150*	*13⅜*	*10,250*
10,250-12,310	*6,310*	*12¼*	*11.3*	*250*	*200*	*11¾*	*12,310*
12,310-17,000	*11,000*	*10⅝*	*12.5*	*300*	*200*	*9⅝*	*17,000*

Cost comparison

Descriptions of past, current and future deepwater Gulf of Mexico activities were acquired from several active operators and used to define the water and well depths, and general geology of three hypothetical wells representative of wells where dual-density systems might be applied. It was concluded that representative wells:

- would be drilled with dynamically positioned rigs;
- would encounter abnormal pressures; and
- would not encounter long salt intervals.

The rigs would be capable of drilling in 10,000ft of water with a 21-in. riser and 18¾-in. (10,000psi) subsea blowout preventer system. The two development wells would be in a water depth of 6,000ft with total depths of 17,000ft and 23,400ft. The exploratory well would be in a water depth of 10,000ft with a total depth of 20,500ft. It should be noted that a significant portion, about 50%, of all future deepwater Gulf of Mexico wells are likely to encounter salt and therefore are not well represented by these wells. Subsalt wells are less likely to benefit from the advantages of a dual-density system and therefore were excluded from consideration.

The data collected also was used as a basis for generic deepwater pore pressure and fracture pressure estimates. The average depth of the top of abnormal pressure for deepwater Gulf of Mexico wells was concluded to be about 2,000ft below the mudline and is independent of water depth. The average local pore pressure gradient in the abnormally pressured section of deepwater Gulf of Mexico wells was found to be about 15.5 lb/gal equivalent. The average fracture pressure in deepwater Gulf of Mexico wells can be estimated using these pore pressures, a compaction-based overburden stress model, and a stress ratio of 0.7. Estimates of pore and fracture pressures based on these averages were used when selecting the mud weights, casing sizes and setting depths as well as hole sizes for the three representative well designs. The resulting well descriptions are reasonably similar to the descriptions of the actual and planned wells in similar water depths that were included in the data industry sources provided. The casing sizes and setting depths for an example conventional well design is summarized in Table 2 for the 17,000-ft deep well in 6,000ft of water. Relatively small kick and trip margins were assumed in the shallower, lower risk section of the well to allow 9⅝-in. production casing to be used.

A "trouble-free" drilling cost estimate was made for each of the three example well designs. The cost estimates assume each well is productive, production casing is run and set, and well operations are suspended pending later completion. Completion costs should not be impacted by dual-density drilling operations and were not included in these cost estimates.

The estimate of recurring daily costs assumes the rig dayrate is $160,000 for all cases.

The additional recurring costs for rentals, services and other support are assumed to be $190,000 per day. Additional point-in-time costs, such as the subsea wellhead, casing, cement, minimal open-hole logging and building an initial mud volume, were itemized and generally represented about 11% of

Table 3. Dual-density, gas-lift well design for 17,000-ft total depth (6,000-ft water depth).

Hole Selection Interval	Depth Below Mudline	Bit Size	Mud Density	Kick Margin	Trip Margin	Casing Outer Diameter	Casing Setting Depth
ft-TVD-RKB	ft-TVD-RML	in.	ppg	psi	psi	in.	ft-TVD-RKB
6,000 (mudline)	0	-	8.6	-	-	36	6,200
6,000-8,000	2,000	26	8.6	0	0	20	8,000
8,010-12,000	6,000	17½	15.2	300	200	13⅜	12,000
12,100-17,000	11,000	12¼	15.4	850	300	9⅝	17,000

the overall well costs. A "trouble-free" drilling time estimate for the single-density well design described in Table 2 is shown in Figure 1. The total time on location is estimated to be 50 days. The corresponding total well-cost estimate is $19.7 million dollars.

The dual-density design for this same example development well is summarized in Table 3. This design represents a significantly smaller trouble risk from a well control and lost returns perspective than the single-density design for the same well because of the larger kick and trip margins.

The same rigs will initially drill dual-density wells as drill conventional wells. The major components required to implement a riser gas-lift system would be nitrogen generation units (10 Mscf/min, 5,000psi), a rotating control head at the surface on the riser, a choke dedicated to the riser and a high capacity mud-gas separation system (300psi, 30 Mscf/min, 2,000 gpm). An additional cost of $60,000 per day is anticipated for these gas-lifting services and equipment rentals during dual-density operations.

Savings from using a riser gas-lift system to drill representative deepwater wells ranged from $2.1 million to $3.3 million or between 9% and 16% without considering the effect of reduced trouble costs.

A trouble-free drilling time estimate for the total time on location for the dual-density well design of the 17,000-ft example well is shown in Figure 2. The total time on location is estimated to be 41 days. This drilling time results in an estimated total well cost of nearly $17 million. The apparent cost reduction realized by using a gas-lift, dual-density well design for this example is about $2.8 million. This would represent a 14% cost savings per well compared with the $19.7 million well cost using conventional single-density methods.

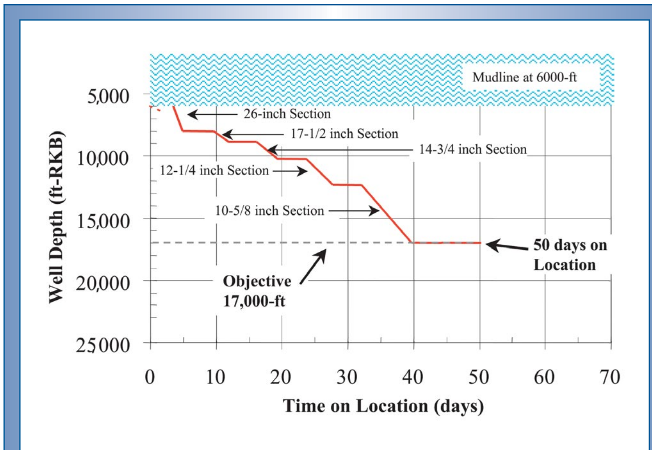

Figure 1. Estimated trouble-free drilling time for conventional 17,000-ft well.

A similar cost estimate was performed for a dual-density well drilled with a liquid dilution system. The casing program was less optimum; additional equipment rentals were $20,000 per day compared with $60,000 per day. Trip and kick margins were only slightly more conservative than for a conventional well, and the cost savings were smaller than for riser gas lift but are still significant at 7%. A summary of all of the cost estimates performed for the three example wells is provided in Table 4. Savings from using a riser gas-lift system to drill representative deepwater wells ranged from $2.1 million to $3.3 million or between 9% and 16% without considering the effect of reduced trouble costs.

Larger savings would be possible if smaller risers were available to extend the water depth limits of smaller, less expensive rigs. Larger savings also could be realized on wells whose depths or pressure profiles would otherwise require more casing strings and from using a wellhead pressure less than the hydrostatic pressure of a column of seawater, which would allow further optimization of the casing program for a dual-density well.

Finally, trouble costs are often a significant portion of deepwater well costs. Although a dual-density system might increase equipment-related downtime and trouble cost, the larger trip and kick margins should eliminate much of the trouble time associated with lost circulation, kicks and extra casing strings often encountered in deepwater drilling. A recent exploratory well drilled in 10,000ft of water exemplified these kinds of problems. Lost returns, flows and related problems consumed 11 days of rig time and increased the well cost by about 15% over the original estimate. An unplanned, extra string of casing also was required to reach total depth. Another case history showed a similar experience. The opportunity for the larger kick and trip margins provided by a dual-density system to reduce these kinds of trouble would reduce deepwater drilling costs. If only half of the trouble described in these examples were eliminated, the well costs would go down by about 8%, bringing the expected overall savings between 17% and 24%. Considering the other potential beneficial impacts of riser gas-lift operations described above, a dual-density well's costs could be as much as 50% less than those for conventional methods to drill the same wells.

Conclusions

Additional research into and development of dual-density systems is needed, particularly for the riser gas-lift approach. Specifically, more comprehensive research should be performed to develop formal procedures for well control and general pressure control during all rig operations, to formalize an overall system design and to determine the probable economics of systems to implement riser gas-lift in deepwater drilling operations.

Riser gas-lift was projected to provide a cost reduction of at least 9%, and more likely between 17% and 24%, of the trouble-free cost for conventional drilling practices for the three example wells selected to represent future deepwater Gulf of Mexico operations. A riser gas-lift approach also increases the feasibility of drilling deep wells in deepwater that might otherwise be impossible with current rigs and equipment. Additional cost reduction can be realized by using smaller risers and rigs. The combined effect could be reductions in actual costs equal to as much as 50% of the estimated trouble-free cost of a well. Riser dilution using liquids is not expected to be as effective for reducing well costs and would reduce costs vs. conventional operations by 7% for the example studied.

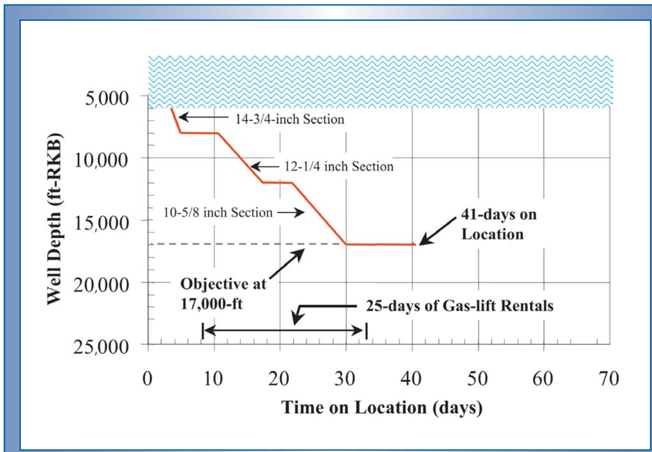

Figure 2. Estimated trouble-free drilling time for a 17,000-ft well drilled with a riser gas lift.

Well control with riser gas-lift was studied and found to be feasible using methods generally analogous to conventional operations and those using a subsea mud lift pump. Kick removal should use returns up a gas-lifted choke line.

Results from this and work done by de Boer indicate that mud separation for a liquid-based riser dilution system is possible. A complete system to accomplish fluid processing with hydrocyclones was not defined but seems feasible.

Average pore and fracture pressure trends in the deepwater sediments of the Gulf of Mexico have been developed. The average depth of the top of abnormal pressure is 2,000ft below the mudline and is independent of water depth. The average local pore pressure gradient below this depth is equivalent to 15.5 lb/gal. The average fracture pressure can be estimated using these pore pressures, an overburden stress model and a stress ratio of 0.7.

Detailed reports on all parts of the project to investigate the feasibility and economics of these dual-density systems are available as publications on the Gas Technology Institute Web site at *www.gastechnology.org* ✧

Table 4. Comparison of single- and dual-density trouble-free cost estimates for deepwater wells.

Example	Total Cost		
	Conventional Single-density	*Riser Gas-lift Dual-density*	*Liquid-dilution Dual-density*
	$ million	*$ million*	*$ million*
17,000ft Total Depth (TD), 6,000ft Water Depth Well	*19.7*	*16.9*	*18.3*
23,400ft TD, 6,000ft WD Well	*23.7*	*21.6*	*Not Estimated*
21,500ft TD, 10,000ft WD Well	*20.5*	*17.2*	*Not Estimated*

Acknowledgements

The authors wish to acknowledge the assistance of the many companies and individuals who contributed to this project. Scandpower provided an academic license for the use of OLGA2000™. Several operators and service companies provided well data. Several drilling fluid vendors provided information and advice, and Fred Growcock and others at MI were especially helpful. Professors Andrew Wojtanowicz and Julius Langlinais, Anamika Gupta, Gerry Masterman and Wayne Manuel at Louisiana State University also contributed to the work described within this article.

Reference

de Boer, L.: DGS Dual-gradient Drilling System, *presentation to the Drilling Engineering Association, Houston, Nov. 20, 2003.*

Putting the Pressure on Fiber Laser Perforations

By Brian C. Gahan, *P.E.,*
Gas Technology Institute

As part of their ongoing investigation into high-power laser applications for well completions, researchers at the Gas Technology Institute were able to perforate steel, cement and rock under high pressure and stress conditions encountered downhole. For the first time, questions about how lasers will operate under real conditions in the field have been answered.

For decades, the use of lasers has continually resurfaced as a quick and easy means of boring through the earth to reach plentiful mineral deposits. Cultural references to lasers or other disintegrating rays emanating from alien spaceships, mountaintop laboratories or handheld weapons have subliminally misled many to believe lasers and photonic energy are infinitely powerful and without limitations. Lasers, of course, are subject to the known laws of physics. Although they have unique capabilities, useful applications for lasers have grown only as technology has advanced. As a result, lasers have been developed to perform multiple tasks across several industries.

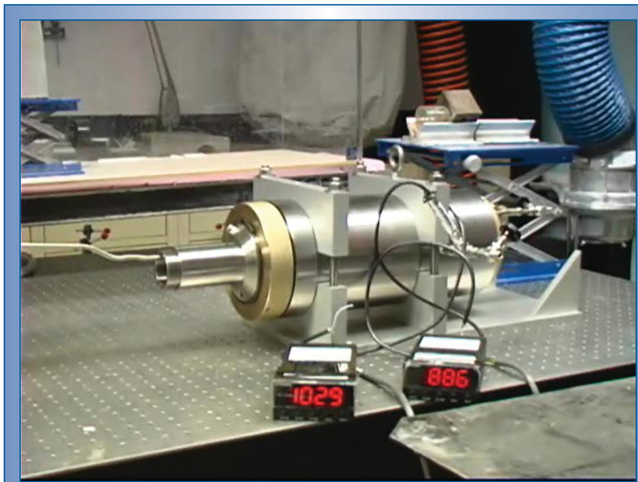

Figure 1. Triaxial pressure cell designed for simulated in-situ laser/rock interaction testing.

Serious investigation of using lasers for cutting and boring through naturally occurring rock is a relatively recent endeavor. Advances in computer technology, control systems and lasers themselves have allowed researchers at the Gas Technology Institute (GTI) to investigate their use as an alternative method for well construction and completion. Several military and industrial lasers with a variety of beam characteristics have been used on an assortment of rock types and other materials to determine the technical feasibility of their use downhole.

High-power fiber lasers represent the next generation for industrial applications offering a number of technical and economic advantages, including higher energy conversion efficiencies; low or no maintenance; and a compact, rugged, solid-state design. They represent an enabling technology that opens the door for laser use in remote field sites, and as such, are considered a leading candidate for near-term subsurface laser applications. (For more information, see *New High-Power Fiber Laser Enables Cutting-Edge Research*, GasTIPS, Spring 2004).

A non-damaging alternative

The oil and gas industry has attempted for years to find acceptable non-explosive alternatives to creating downhole reservoir connectivity with the wellbore. Although some methods have proven capable in providing an economic and technical solution, the use of shaped charges remains the preferred technology for most applications.

Shaped charge explosives have drawbacks upon which alternative perforation methods seek to improve. A prime example is the crushing of the rock matrix near the tunnel zone from the jet's high velocity mass transfer, resulting in a significant reduction of flow from the reservoir into the wellbore. Remedial work with some form of stimulation often is required to overcome this flow restriction. Other concerns voiced by the industry include the inherent safety challenges regarding the transportation, storage and use of the perforating assembly. Regulatory concerns also focus on limitations that may be raised on the use of explosive charges, challenging the industry's ability to economically complete wells around the world.

The application of high-power lasers to create the path between the wellbore and reservoir could significantly reduce the primary drawbacks of using explosives. In addition to perforating, laser applications could perform other on-site tasks, including cutting windows for side exiting casing or laterals, extended perforations that connect additional reservoir rock to the wellbore and removal of objects lost downhole that would normally require drill out or fishing operations.

Laser perforation experiments in the past have been performed using combinations of laser input parameters on several rock lithologies to determine specific cause and effect relationships. Optimized variables were identified and demonstrations conducted to show the capability of lasers to cut tunnels of at least

12-in. deep into sandstone and limestone. One notable advantage resulting from laser perforation on sandstone is the improvement of near-tunnel fluid flow characteristics. Measured permeability increased between 15% and 30% along the tunnel face of a perforation demonstration on a 12-in. block of Berea sandstone.

Perforating under pressure

Although the application of lasers for perforation provided promising results, downhole pressure conditions had not been investigated. All high-power laser application experiments performed to date had been conducted under ambient pressure conditions in the laboratory. To perform high-pressure tests on rock, a triaxial pressure cell was designed to allow multiple pressure conditions, a simulated pressurized wellbore, a window for the laser beam to interface with the sample and ejection ports for lased material.

As part of a recent laser perforation study, tests were conducted with the triaxial pressure cell to give an initial understanding about how high-pressure conditions similar to that found downhole influence the laser/rock interaction process. The laser used in this experiment was a 5.34-kW ytterbium-doped multiclad fiber laser with an emission wavelength of 1.07 microns. The triaxial pressure cell rated at 3,000psi was designed for this experiment to allow laser beam exposure to a 4-in. diameter by 6-in. in length pressure-charged rock core by means of a sapphire window.

Between the window and the core is a chamber that simulates a wellbore and can be independently charged with pressure to simulate over-balanced conditions. At-balance conditions are simulated with ambient pressure in the wellbore chamber and no pore pressure in the rock sample. Underbalanced conditions are simulated with ambient conditions in the wellbore chamber and pore pressure in the rock sample.

Ports in the wellbore chamber allow ejection of cuttings and other materials. The design of the wellbore chamber minimizes the exposure of the optics to all material ejected from the sample during the lasing process. The design has proven successful in this application and will be incorporated in future field prototype tool designs. A photograph of the completed high-pressure cell is shown in Figure 1.

Pressure test on rock core

Initial tests were performed on cores of Berea sandstone and Indiana limestone under various conditions of axial, pore and confining pressures. The laser settings remained constant for all cases. Full output power of 5.34 kW was applied continuously to each sample through the sapphire window of the pressure cell with a beam diameter of 0.35-in. for 8 seconds. The amount of laser exposure time was calculated from previous laser rock interactions to allow penetration into the core without risk of penetrating the core's full length and avoiding possible damage to the pressure cell.

Five trials were performed on unsaturated samples of each rock type. A base case was established for each rock type by lasing samples in the cell at ambient pressure conditions. A second condition was tested on each rock type with confining and axial stress limited to about 1,000psi. Since the cores were not charged with pore pressure, a high-pressure gas purge of 90psi through a quarter-in. nozzle assisted in particle removal.

A third condition was then tested for each rock type that combined confining and axial stress limited to about 1,000psi, while charging the core to a pore pressure. No gas purge was provided as underbalanced conditions (greater pore pressure than wellbore pressure) served to eject particles from the charged core through pressure cell exit ports. Two additional trials were performed at balanced and underbalanced conditions with double the pressure settings.

To better understand the *in-situ* performance of lasers in the presence of reservoir fluids, sandstone and limestone cores were saturated in brine and liquid hydrocarbon prior to high-pressure lasing. Pressure conditions for each rock type included confining and axial stress limited to about 1,000psi with no pore pressure. Results of all high-pressure core tests are presented in tables 1 and 2.

Pressure tests on composite core

After observing the laser/rock interactions of

Table 1. High-pressure cell tests on Berea sandstone.

Trial Number	Conf. Pressure (psi)	Axial Pressure (psi)	Pore Pressure (psi)	Volume Removed (cc)	Specific Energy (kJ/cc)
B1	0	-	-	2.03	19.75
B2	1,120	1,180	-	2.53	15.80
B3	1,101	1,106	864	1.97	20.31
B4	2,031	2,000	-	2.44	16.38
B5	2,100	2,215	1,565	3.10	12.91
Brine	1,893	1,991	-	5.45	7.84
Oil	1,844	1,956	-	1.60	26.76

Table 2. High-pressure cell tests on Indiana limestone.

Trial Number	Conf. Pressure (psi)	Axial Pressure (psi)	Pore Pressure (psi)	Volume Removed (cc)	Specific Energy (kJ/cc)
L1	0	-	-	0.40	99.97
L2	1,029	1,139	-	0.93	43.00
L3	982	1,056	864	1.02	39.04
L4	2,069	2,169	-	0.98	40.67
L5	2,100	2,225	1,625	3.26	12.27
Brine	1,922	1,981	-	1.87	22.78
Oil	1,800	1,930	-	0.85	50.36

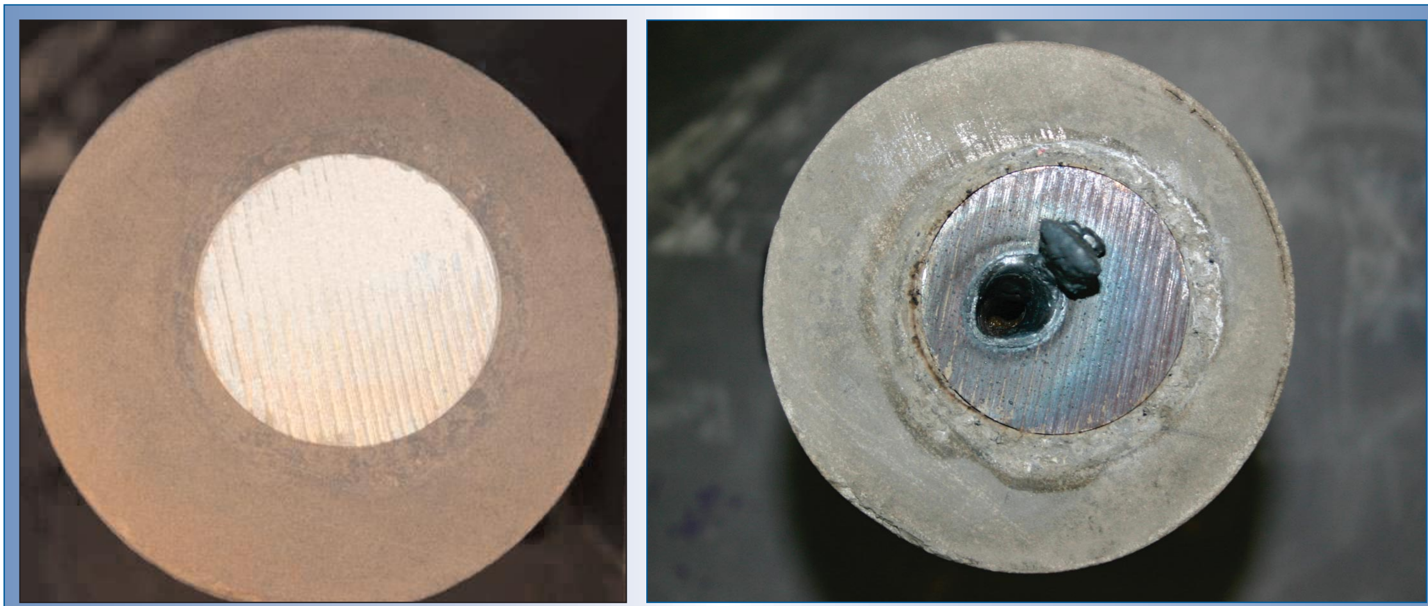

Figure 2. Pre- (left) and post-lased images of 4-in. by 6-in. limestone core inset with 2-in. by half-in.-thick steel plate.

sandstone and limestone under high-pressure conditions and the resulting specific energy values, *in-situ* demonstrations were then executed to best simulate downhole conditions and material encountered during laser perforation. Composite samples of steel, cement and rock were prepared by cementing in place a 2-in. diameter by half-in.-thick steel plate. By using a smaller steel diameter inset, the rubber pressure sleeve jacketing the sample core would not be at risk of melting through direct contact with a full diameter steel plate.

The sandstone and limestone clad samples were exposed to the same laser beam conditions as performed under previous high-pressure trials. For the sandstone sample, axial and confining pressures were measured at 2,100psi and 2,030psi, respectively. Axial and confining pressures for the limestone sample were measured at 2,074psi and 1,966psi, respectively.

Total time of beam exposure was 90 seconds per composite sample. The time was calculated based on earlier laser exposure times to remove a unit volume of steel, cement and rock materials. The laser fired for 30-second intervals buffered with 20 seconds between shots as a precaution to avoid overheating the cell assembly. Before and after lasing images of the limestone clad sample are shown in Figure 2.

As a result of the high-pressure clad sample trials, the laser penetrated about 2½-in. into the sandstone clad sample, or a half-in. beyond the steel and cement. The laser penetrated 4½-in. into the limestone clad sample, or 2½- in. beyond the steel and cement. An X-ray CT scan image of the limestone clad sample is shown in Figure 3.

Pressure test results

The resulting data generated from the series of sample trials on sandstone and limestone have demonstrated that a laser perforation system will significantly benefit from the high-pressure conditions encountered downhole. For both rock types, specific energy values decreased as confining and axial stresses increased. The effect was more apparent in the limestone than in the sandstone samples.

Sandstone—The removal mechanism for Berea sandstone is spallation, where rapid differential thermal expansion causes grains and cementitious material to fracture. The base case for sandstone with no pressure had an SE value of 19.75 kJ/cc. The conditions are similar in many respects to much of the previous work performed in the lab. The sample is at ambient conditions during lasing and a gas purge nozzle assists in removing broken material.

The lowest SE value observed in sandstone was 12.91 kJ/cc, a 35% reduction from the base case, resulting from the highest-pressure values tested. Material removal was assisted with the differential between the pore pressure and wellbore chamber pressure. As this differential increases, material is more rapidly ejected from the tunnel, thus minimizing travel through the cutting beam and absorbing less beam energy after detaching from the rock matrix. With less beam energy absorbed by exiting particles, more is available for cutting, as evidenced by the drop in the SE value.

At the pressures tested, confining and axial stress had a limited impact on SE values for sandstone. The stresses imparted on the sandstone matrix create tighter grain-to-grain contact and improved the thermal diffusivity of the rock. In both cases, material is purged with an assist gas with the same conditions for each trial.

Limestone—The removal mechanism for limestone is calcination where the energy of the laser beam causes a thermal dissociation of carbonates into carbon dioxide and calcium oxide (lime). Just as axial and confining stress compressed the sandstone, the effect was more evident in the limestone samples. This quarry limestone was originally unstressed, contributing to an SE drop of at least 60% because of closer grain-to-grain contact and a more efficient calcination process.

The lowest SE value was observed in limestone at the highest pressure and stress conditions. Again, the differential pressure assisting in material removal was evident with a significantly lowered SE of 12.27 kJ/cc, 88% lower than the base case.

Conclusions

High-power laser applications for cutting and boring rocks have been successfully demonstrated under ambient pressure conditions; however, this is the first time samples have been lased at *in-situ* pressure conditions. Research results demonstrated the beneficial effect of stress and pressure on the laser's ability to perforate reservoir rock. Additionally, we were able to demonstrate the capability of a single wavelength laser to penetrate a combination of steel, cement and rock at *in-situ* pressures that would be encountered while perforating downhole.

Operating the laser in underbalanced conditions showed the laser's ability to perform at downhole conditions without requiring a supplemental assist purge system. The differential pressure between the reservoir pore pressure and the wellbore pressure provided the means for ejecting the cuttings.

Operating the laser on rock under axial and confining stress improves the conditions for laser perforation because of a closer grain-to-grain contact and resulting improvement to thermal diffusivity. This extends the influence of the beam energy further into the rock.

Looking ahead

Additional research has been proposed to follow on our initial *in-situ* pressure investigation. Questions remain about how best to transmit energy downhole, effects of higher pressures on the lasing process, energy application on the target and whether any fluid flow improvements result from a lased perforation tunnel.

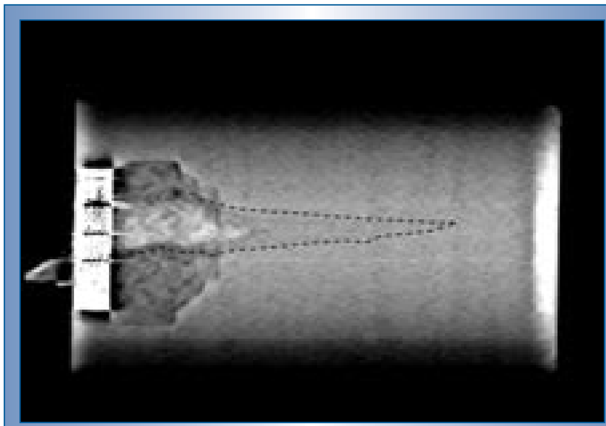

Figure 3. CT scan image of 4-in. by 6-in. limestone clad sample and outline of penetration path after perforation of three 30-second shots by a 5.34-kW ytterbium fiber laser with a 0.35-in. diameter beam.

A better understanding is required of high-power laser energy transmission from the surface to the reservoir. Energy losses, or attenuation, of low-energy transmission over long distances through solid-core silica fiber are better understood than with high energy transmission. As a result, we need to determine whether a correlation exists between the calculated attenuation losses at low power with those observed at high power. Associated with these energy losses is the need to better understand how lost energy is dissipated and whether there are any negative effects on the physical and light transmission characteristics of the silica fiber.

Although we got our first look at high-pressure lasing of rock, additional experiments should be carried out at higher pressures. A series of experiments can be performed on rock and clad samples, such as steel, cement and rock, at pressures and stresses beyond that previously achieved. We believe the system will continue to behave favorably at greater depths and would like to determine this by lasing samples under pressure and stress conditions simulating at least 15,000ft.

Energy losses at the working surface also require investigation. Experiments on fluid behavior at downhole pressures and temperatures could determine distance limitations because of energy absorption by fluids. In addition, it should be determined how well different gas and liquid purging fluids can extend the effective lasing distance through reservoir fluids.

It has been shown that high-power laser applications avoid damage and can improve the porosity and permeability of rock in the perforated tunnel and adjacent zones. Although these enhancements suggest production from a laser perforation should outperform production from an explosive perforation, no comparative tests have been performed. Core flow measurements could be performed and results correlated with lasing conditions and input parameters, including beam shapes and intensity, *in-situ* pressures and stresses, and the effect of lasing across pressure differentials.

The issues addressed in upcoming research should allow the initial design of a downhole prototype tool. Researchers are hopeful that field experimentation will soon follow. If successful, the door will have opened further to other remote site laser applications. ✧

References

1. *Gahan, B.C., et al.* Laser Drilling: Determination of Energy Required to Remove Rock, *SPE Paper No. 71466,2001.*

2. *Gahan, B.C., Batarseh, S., Sharma, B., Gowelly, S.* Analysis of Efficient High-Power Fiber Lasers for Well Perforation, *SPE Paper No. 90661, 2004.*

3. *Batarseh, S., Gahan, B.C.* Deep Hole Penetration of Rock for Oil Production Using Ytterbium Fiber Laser, *SPIE Paper No. 5448-98, 2004.*

Field Tests of TR650 Squeeze-off Tool Successful

By Kenneth H. Green,
Timberline Tool

Timberline's TR650 squeeze-off tool or above-ground repair of polyethylene pipe between 3-in. and 6-in. diameter is commercially available following successful completion of laboratory and field tests.

Natural gas is a widely used, clean and efficient fuel, and its consumption is growing (Figure 1). Natural gas utilities operate and maintain more than 1.2 million miles of underground pipes for delivery of natural gas, according to reports by the American Gas Association. Polyethylene (PE) pipe constitutes the majority of gas distribution piping installed in the United States today.

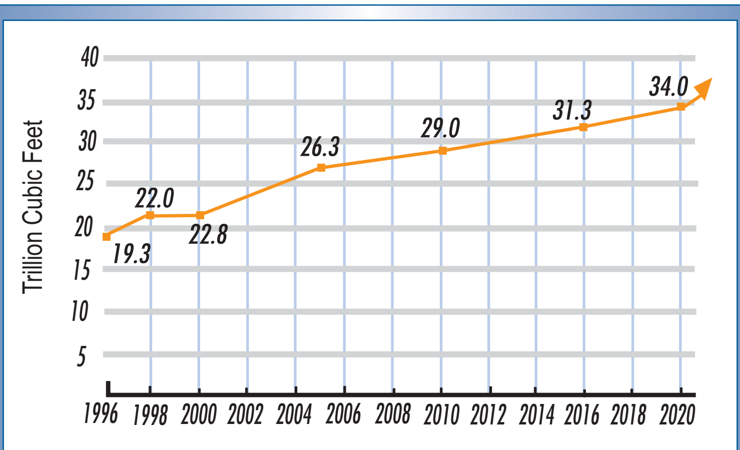

Figure 1. U. S. Department of Transportation forecasts a 50% increase in natural gas consumption by 2020.

The U.S. Department of Transportation forecasts a 50% increase in the demand for natural gas by 2020. It is important to maintain the existing and growing infrastructure to ensure the safe and reliable delivery of natural gas in the future.

The report titled *Natural Gas Infrastructure Reliability—Pathways for Enhanced Integrity, Reliability and Deliverability*, developed by the U. S. Department of Energy/Office of Fossil Energy and the National Energy Technology Laboratory, draws attention to the need for improved tools for the construction, maintenance and repair of the gas pipe that makes up the majority of America's natural gas distribution network. This report cites a preference for cost-effective and efficient tools to facilitate repair through "keyhole" excavation access, providing significant safety and cost advantages over backhoe-style excavations. With the financial assistance of the Department of Energy through a Small Business Innovation Research Award and cost-sharing support from natural gas industry companies, Timberline Tool was able to develop its TR650 specifically designed for repairing large-diameter plastic pipe in keyhole situations.

Similar to arthroscopic surgery, keyhole access technology allows the buried natural gas pipe to be accessed and squeezed-off or repaired through a small (18-in. diameter) keyhole above the pipe. It eliminates the need for extensive and disruptive excavation with a backhoe or other large equipment at the repair site (Figure 2).

Timely repair of a leaking natural gas pipeline is of critical importance to the safety, reliability and cost effectiveness of the United States' natural gas pipeline system. The important first step in any gas line repair is to stop the flow of natural gas. Squeeze-off is a procedure used to temporarily shut-off the flow of gas in the pipeline to facilitate maintenance or repair operations. During the squeeze-off procedure, the pipe is compressed between two bars until the flow of gas within the pipe stops. After the maintenance or repair to the gas line has been completed, the bars are released and gas flow through the line resumes. In June 2002, Timberline Tool began to develop a mechanical tool to squeeze-off between 3-in. and 6-in. PE pipe using keyhole technology (Figure 3).

Squeeze-off tools are available for use on smaller natural gas pipes (between a half-in. and 2-in.) for traditional and keyhole excavations. However, squeeze-off tools for repair of larger gas pipes (between 3-in. and 6-in.) through 18-in. keyhole access were not available until the recent development of Timberline's TR650, which enabled squeeze-off to be performed from the top-down, in one simple operation. By squeezing-off PE pipe from the top-down, substantial time and labor costs associated with extensive excavation are reduced.

Recent field evaluations of the tool at several natural gas companies (Figure 4) demonstrate advantages over traditional squeeze-off tools for natural gas between pipe 3-in. and 6-in. The tool's new design is lightweight, a single operator can manage it, and it and keeps workers out of the trench.

KeySpan Energy and NW Natural estimate the tool will generate savings per excavation of more than $1,000 compared with traditional excavations. Each of these companies performs between 500 and 1,100 squeeze-offs in their territory per year.

"Our existing keyhole program for service installation and main inspection has been successful, but this type of tool will expand our capabilities tremendously," said George Gent, NW Natural's manager of construction and technical services.

During Phase 1, the feasibility of the TR650 was demonstrated successfully to utilities cited in Figure 4. This new keyhole squeeze-off tool concept for PE pipe between 3-in. and 6-in. is a natural fit for Timberline Tool's product line, which includes TopReach squeeze-off tools in use for PE pipe between a half-in. and 2-in. for access holes as small as 18-in. in diameter.

Significant research and development in Phase 2 provided optimal design characteristics and operational procedures for the engineered prototype. The approach in both phases included detailed engineering analyses, and rigorous and carefully controlled laboratory tests and field tests in preparation for commercialization.

The anticipated public benefits include safety of workers and neighborhoods, reliable squeeze-off and cost effectiveness. The tool's remote operation keeps the worker out of the trench and away from blowing gas, and operates through keyhole access without the need for large excavations. Operators are able to perform the repair work more quickly and in smaller areas decreasing the chance of danger to themselves and others in the area. The tool is built from high strength, non-sparking aluminum alloy.

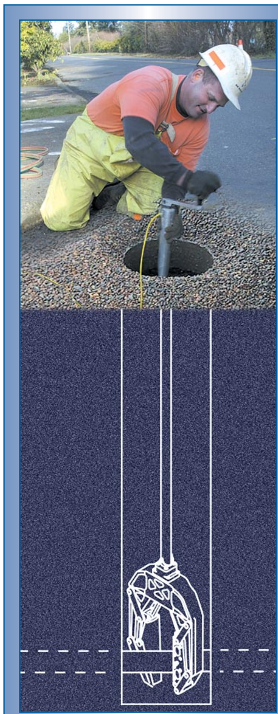

Figure 2. Timberline's "keyhole" solution for PE pipe repair.

Why Keyhole Technology?

Cost-Saving Alternative to Conventional PE Pipe Repair Methods

Conventional Method	Timberline Keyhole Method
Operators work in trench.	Operators work above ground.
Requires large "open" excavations.	Requires single "keyhole" excavation.
Requires multiple operators & operations.	Requires one operator, one operation.
Requires excavation under the pipe.	Under-the-pipe excavation not required.

Figure 3. Keyhole technology increases safety, saves labor and time and provides significant cost savings.

Company	Location
NW Natural	Portland, OR
Sempra Energy Utility	San Diego & Los Angeles , CA
Questar Gas Company	Salt Lake City, UT
Southwest Gas Corporation	Tempe, AZ & Las Vegas, NV
Nicor Gas	Naperville, FL
DTE Energy (MichCon)	Melvindale, MI
KeySpan Energy Delivery	Hicksville, NY
Oregon State University	Corvallis, OR

Figure 4. Natural gas companies participating in the field evaluations of Timberline's TR650.

The new squeeze-off tool demonstrated reliable squeeze-off when field-tested by partners on PE pipe between 3-in. and 6-in. diameter. Utility operators were consistently able to squeeze-off the pipe without inducing damage. The tool was designed and built to apply limited pipe compression so it cannot over-squeeze the pipe; operators can control the squeeze-off and release rate preventing pipe damage. The squeeze tool geometry, such as 4-in. squeeze bar radius, enables reliable squeeze-off with less pipe compression. The tool is designed to automatically center the pipe in the jaws, eliminating visual guidance or other means to ensure proper positioning for a safe squeeze-off. The screw actuating mechanism in the tool prevents uncontrolled quick release that could damage the PE pipe.

Current procedures for repairing buried natural gas pipe are time consuming and expensive. The TR650 squeeze-off tool operates through keyhole access and provides cost savings by reducing squeeze-off time, reducing the size of the excavation required for squeeze-off, reducing the pavement restoration effort, increasing productivity with a single operator performing the repair, and increasing the efficiency of the overall squeeze-off and repair process, which will result in less labor hours and unaccountable gas loss.

This project resulted in a mechanical squeeze-off tool that will substantially lower the time and cost of repairing gas distribution piping between 3-in. and 6-in. diameter. This

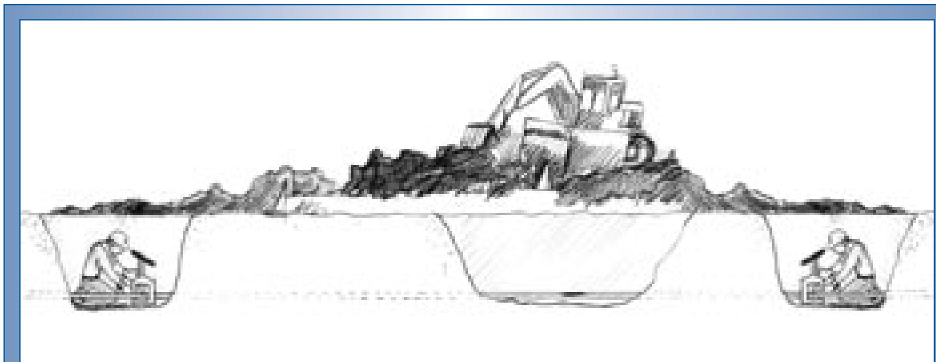

Figure 5. Conventional method for repairing large-diameter distribution lines.

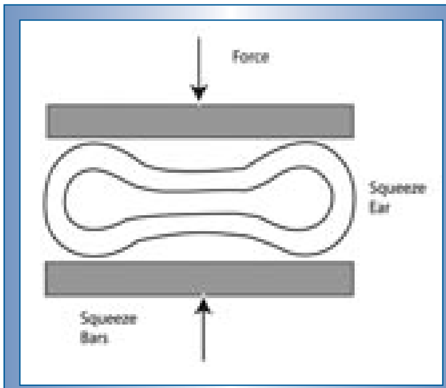

Figure 6. Definition of wall compression.

shows substantial cost savings when using keyhole repair compared with the current operating procedures that require backhoe excavations and heavy equipment to perform the repairs (Figure 5).

The successful demonstrations of the keyhole squeeze-off tool at natural gas utility test sites, the enthusiastic response of utility representatives, and the supporting laboratory tests and analyses provided evidence for technical feasibility. Initial research for this new technology centered on determining the optimum squeeze bar configuration. When PE pipe is being repaired, it is squeezed to prevent gas leakage. Tests were performed to determine the amount of force required to bring the pipe to different degrees of compression with varying parameters such as temperature, squeeze rate and jaw size. Percent compression is defined by the following equation in ASTM F1734-96 (Figure 6).

% Compression = (1-L/2t)

Where L = Jaw gap and t = average wall thickness expressed in the same units as L.

MDPE 2406 SDR 11.5 gas pipe samples were tested in steel jaw fixtures placed in a MTS hydraulic testing frame. A 150,000-lb capacity strain gauge was placed between the hydraulic cylinder and the connection to the top jaw. The bottom jaw was stationary on the blocks placed on the framework table, and the deflection measurements were made in the head of the hydraulic unit. In most cases, two identical runs were made with two different pipe samples. MDPE pipe samples were 2ft and 3ft long for the 4-in. and 6-in. pipe diameters. Pipe samples were temperature equilibrated for at least 24 hours prior to testing.

Steel jaw assemblies were made with 2½-in., 3½-in. and 4½-in. jaws. All jaw major profiles were 4-in. radius, while the edge radius was one-quarter-in. with the exception of early 2½-in. jaw runs where the edge radius was 0.06-in. The 2½-in. jaw was of a fixed design only while the 3½-in. and 4½-in. jaws were used in a fixed and swivel configuration.

The force and deflection data gathered for each run was inspected to find the "linear" region once wall contact was achieved. The force range typically used was between 12,000 lb and 34,000 lb for the 4-in. pipe while between 18,000 lb and 34,000 lb were used for the 6-in. pipe. Second order polynomials were fitted to these ranges for each run. To account for the deflection of the test frame and the jaws, a run was made for each configuration (with no pipe samples) to find the force/deflection values for the entire range (between 800 lb and 36,000 lb). This structural deflection data also was fit to a polynomial.

Duplicate runs were compared and all were reasonably consistent. To calculate the force required to squeeze the pipe to 5%, 10%, 15% and 20%, the equations of any duplicate runs were averaged and the equation for the amount of deflection was subtracted. The resulting new equation was used to generate "true" deflection data for between the 12,000-lb and 40,000-lb force range for each jaw configuration and pipe size. Once again, this data was fit to a polynomial. These final equations were used to calculate the 5%, 10%, 15% and 20% values that are plotted on the 68.7°F 4-in. and 6-in. pipe graphs (figures 7 and 8).

Increasing the jaw width results in a less vertical incline on the wall compression curves. Initially, more force is required to squeeze the pipe until both walls touch. At this point, the force required to compress the walls lessens.

Once the optimum squeeze bar configuration was determined, various conceptual tool designs were developed to accommodate the squeeze bars and incorporate the following design criteria:

- direct approach from above the pipe;
- parallel clamping motion;
- controlled rate of closure and release;
- manual one-person operation;

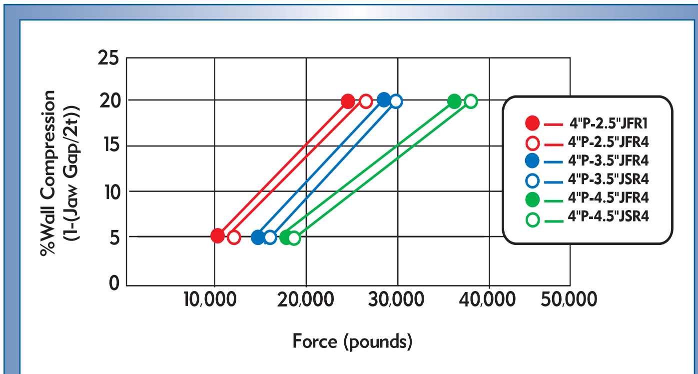

Figure 7. Force required to achieve desired percentage of wall compression for 4-in. MDPE pipe at 68.7°F.

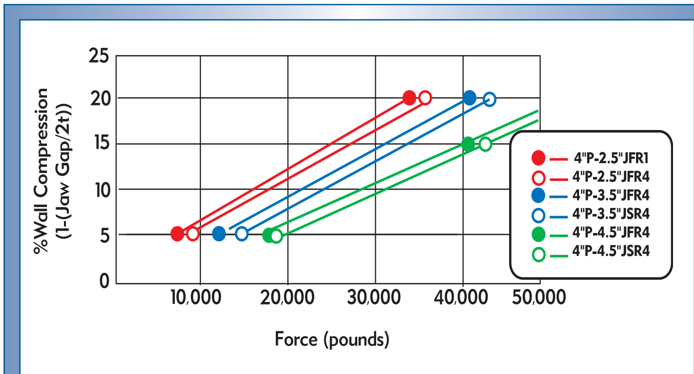

Figure 8. Force required to achieve desired percentage of wall compression for 6-in. MDPE pipe at 68.7°F.

- stop the flow of gas without pipe damage;
- multiple pipe sizes on one tool;
- ability to withstand the forces generated during squeeze-off;
- lightweight and portable; and
- accommodates "lockout/tagout."

The double actuated design (Figure 9) was preferred over other concepts because both jaws are actuated at the same time, producing only horizontal motion relative to each other. The only sliding part of the tool is the actuator, which is contained within the frame, reducing its exposure to contaminate.

The yoke (Figure 10) is constructed from a single piece of 4-in.- thick 7075-T6 aluminum and designed to provide up to 30,000 lb of crushing force to a 6-in. PE pipe without suffering deformation. Cosmos software was used for performing the stress analysis on the yoke. Figure 11 shows how symmetry allows half of the yoke to be modeled to simplify the numerical solution. A free-body diagram of the jaws in the closed clamp position shows the 30,000-lb crush force will always divide equally between the top and bottom pins on the yoke. Thus, a 15,000-lb load was applied horizontally to each hole in the yoke. The two surfaces at the plane of symmetry are restrained by material on the other half of the yoke. The high stress concentration areas in the yoke are predictably in the fillets on the inside of the yoke (Figure 12). Dividing the yield stress by the maximum stress in the part (73,000/ 57660) gives a 1.266 safety factor for the yoke when manufactured from 7075-T6 Aluminum.

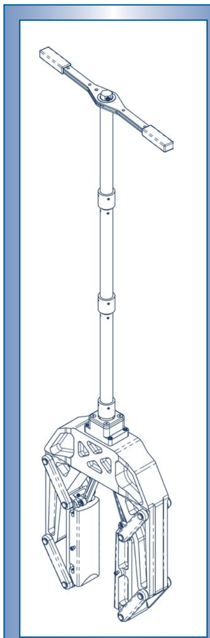

Figure 9. Preferred double-actuated design concept for achieving squeeze-off of between 3-in. and 6-in. PE pipe.

Figure 10. Computer model of the Timberline TR650 yoke.

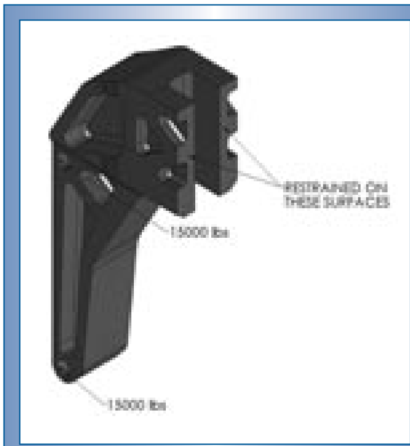

Figure 11. Symmetry of the TR650 yoke simplifies numerical solution.

Figure 13a shows the exaggerated shape of the yoke under load. Since the model is only half of the yoke, the actual measured deflection across the tips of the yoke is double the 0.460-in. This prediction has been correlated to actual measured deflections across the tips when squeeze-off was achieved on a 6-in. pipe. This deflection will be in the elastic range and will return to zero when the clamping load is released.

Following completion of the computer modeling for the components of the TR650, nine engineered prototype tools were manufactured with interchangeable jaws, which permit use of the same tool on PE pipe between 3-in. to 6-in. diameter. These tools are being field tested and evaluated by natural gas companies in various geographic locations. They are being tested for functionality, ease of use and ergonomics. In addition to the functionality tests performed on the prototype delivered to Oregon State University (OSU), sections of the pipe squeezed-off during natural gas company testing were sent to OSU for evaluation of operability in general accordance with *ASTM F1563-01, Standard Specification for Tools to Squeeze-off Polyethylene (PE) Gas Pipe or Tubing*, and *ASTM F1734-96 Standard Practice for Qualification of a Combination of Squeeze Tool, Pipe, and Squeeze-off Procedure to Avoid Long-Term Damage in Polyethylene (PE) Gas Pipe*.

Three specimens each of 4-in. and 6-in. diameter PE pipe were prepared, squeezed and held for 30 minutes. The rate of leakage, if any, was determined using a calibrated rotameter (flowmeter) with 100psi nitrogen supplied to the specimen. Various dimensions were obtained during the procedure.

In addition to inspection procedure within ASTM F1734, the interior and exterior surfaces of the pipe were inspected using scanning electron microscopy at the squeeze ear locations (drop-shaped areas of the pipe created as the walls of the pipe are compressed toward each other).

The remaining specimens were nondestructively inspected on the exterior only. The two remaining 6-in. specimens and one of the remaining 4-in. specimens were then pressure tested.

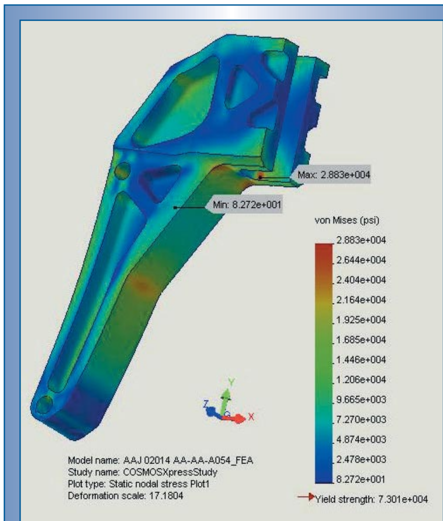

Figure 12. Cosmos computer solution of TR650 yoke under stress.

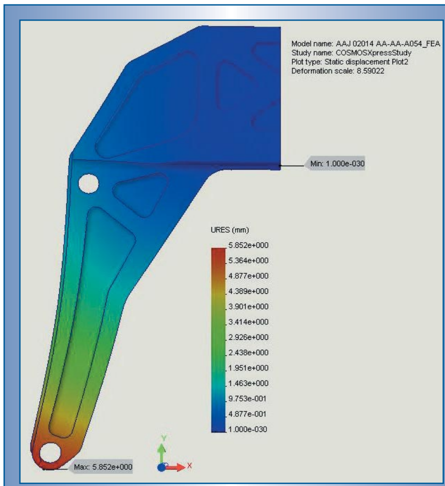

Figure 13a. Cosmos computer solution of TR650 yoke under extreme stress.

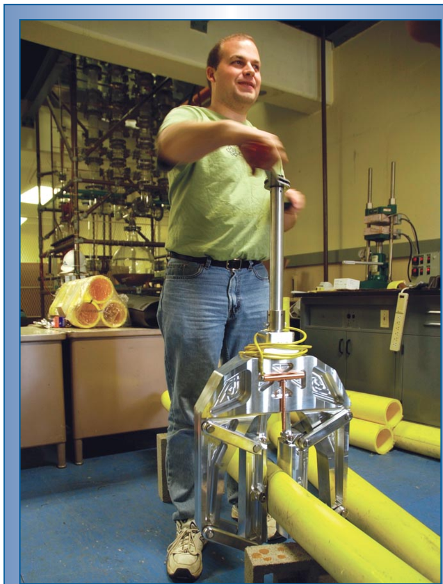

Figure 13b. Successful laboratory testing of TR650 on 4-in. MDPE pipe according to ASTM F1563, the standard specification for tools to squeeze-off PE gas pipe or tubing.

The results of testing to ASTM standards are summarized below.

ASTM F1563 Testing—The squeeze-off tool was evaluated for release protection, release rate, flow control, grounding, squeeze-bar configuration, over-squeeze protection and squeeze bar spacing. Evaluations showed the force could only be released by unscrewing the tool. The operator controls the rate of release manually. The tool has a specific location and attachment for grounding. The 4-in. radius squeeze bar exceeds the minimum 1-in. specification. The actual squeeze percentages (wall compression) were significantly less than specifications. The lengths of the squeeze bars were sufficiently long enough to squeeze-off between 4-in. and 6-in. pipe (Figure 13b).

ASTM F1734 Testing—All squeezed specimens subsequently pressure tested and microscopically tested were inspected per ASTM F1734. There was no evidence of a dimple present on the exterior surface of the squeeze ears. A dimple is a slight indentation or depression in the wall of the PE pipe indicative of serious interior cracking. After sectioning to expose the interior surface of the squeeze and visually inspecting, there was no evidence of stress whitening, crazing or cracking. Some wrinkling was present on the interior surface of the squeeze ears. Some wrinkling and stress whitening is expected to occur, according to ASTM F1734.

Additionally, the interior squeeze ear surfaces were inspected using optical stereo microscopy at 10X magnification, and no evidence of cracking or voids was found. There was no evidence of stress whitening present when inspected at magnifications up to 10X. There also was no evidence of changes in color. After these inspections were performed, the squeeze ear was cross-sectioned and inspected for the presence of subsurface voids in the squeeze area and none were found.

The results of these tests confirmed the effectiveness of the TR650 to squeeze-off between 3-in. and 6-in. PE pipe without changing its integrity. The tests at OSU showed complete squeeze-off occurred at about 5% compression, well below the test tool design value of 15%.

The project team designed, constructed and tested the TR650 squeeze-off tool for large-diameter PE pipe (Figure 14). This tool met or exceeded all of the performance goals. Field evaluation and testing demonstrated the feasibility of using the new squeeze-off tool to effectively squeeze-off between 3-in. and 6-in. PE pipe in keyhole situations without damaging it. The natural gas industry personnel's response to participate in this keyhole squeeze-off tool project further demonstrates its success.

"There is absolutely a strong need for this in the field," said Don Brost, a construction quality assurance supervisor at Northwest Natural. "This is the best we've found of its kind." ✧

Acknowledgements

Funding for this project was provided through a Small Business Innovation Research Award, DE-FG02-03ER83858, by the U.S. Department of Energy (DOE) and managed by the National Energy Technology Laboratory (NETL). Timberline Tool thanks the DOE and the NETL for their financial, technical and administrative assistance in funding and managing this project. The author would also like to thank Oregon State University, KeySpan Energy, DTE Energy (MichCon), Nicor Gas, NW Natural, Questar Gas Co., Sempra Energy (Southern California Gas & San Diego Gas & Electric) and Southwest Gas Corp. for their support for this project.

For more information, contact Ken Green at khg@timberlinetool.com *or (406) 755-4258.*

Figure 14. Pipe integrity maintained following squeezed-off on 6-in. MDPE pipe with the Timberline TR650.

Improving Formation Evaluation and Exploration in Low-permeability Reservoirs

By Randal L. Billingsley, *Advanced Resources International Inc.* and Maria Wood Henry, *Henry GeoConsulting Services*

A key factor affecting the economic viability of some low-permeability reservoirs in the Rocky Mountains is the occurrence of mobile water at reservoir depths, sometimes in large quantities. Understanding the nature and mobility of fluids in these settings is an important aspect of determining original gas in place, and controlling the cost of finding and development in marginally economic accumulations.

Advanced Resources International Inc., with support from the U.S. Department of Energy, is performing a research program (DE-FC-02NT41437) to characterize the nature, distribution and flow paths of moveable fluids in the subsurface of the Greater Green River (GGRB) and Wind River basins (WRB). The goals of this project are to improve resource characterization, develop water remediation strategies and enhance gas recoveries in these resource-rich basins.

The initial project objective was to assemble a digital database of existing produced water chemical analyses performed by operators throughout the exploration and development history of the basins, and data was compiled from a number of private and public sources. While considerable information existed about produced water chemical composition, the information was difficult to access because of multiple formats, duplication, uncertain locations and other factors. Compilation of this data into a single database, with removal of duplicates and invalid analyses, opens the data to access by a broad audience of users with interests in resource assessment, formation evaluation, prospect generation and exploitation of tight formation gas.

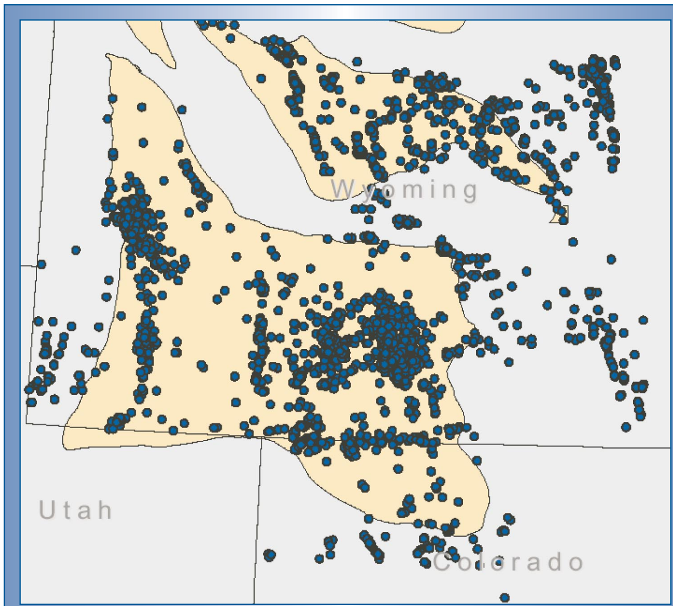

Figure 1. Distribution of sample locations for the produced water chemistry database.

The water chemistry database was assembled for the GGRB and WRB. General coverage is shown in Figure 1. The database includes more than 8,000 compositional analyses from 3,200 wells that can be sorted by various criteria, including geographic area, formation (of record) and test type. Data were screened for analytical validity of compositional data using standard industry practices. Most historical data samples include standard seven-component analyses. In addition, new samples included stable and strontium isotope analyses, and were collected from Waltman/Cave Gulch fields (WRB), and Pinedale, Table Rock and Wild Rose fields (GGRB) for a total of 85 wells. Although the analyses were screened for chemical validity, formation tops and other data were accepted into the database as originally provided by operators; therefore, users must assess suitability of the data for their own purposes.

The database is available for download in three common digital formats from the National Energy Technology Laboratory Web site (*www.netl.doe.gov/scngo/*, see projects link). Individual entries contain any available supporting documentation and intervals as reported by the operator. An attempt was made to lump formation intervals across the database so regional scoping maps can be constructed.

The final product of the project (available next month) will be a digital atlas with regional and local maps of interest and a series of local studies demonstrating uses of the data and potential implications on the broader issues of basin centered gas.

The digital database format allows nearly limitless options to query and sort the data. Once the database has been attached or loaded to a software package with mapping

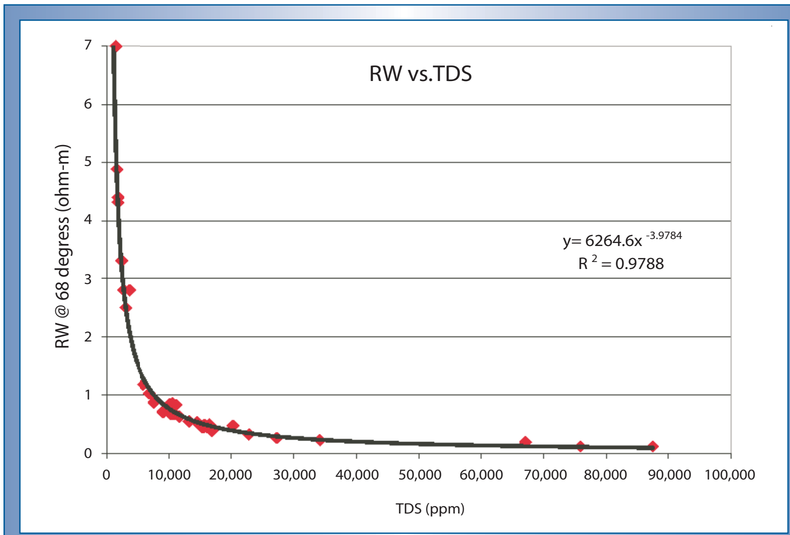

Figure 2. Resistivity of produced waters has not always been measured. A digital database allows a relationship to be constructed between a commonly available attribute, total dissolved solids and resistivity. This relationship can then be used to estimate resistivity for samples where the attribute was not originally measured.

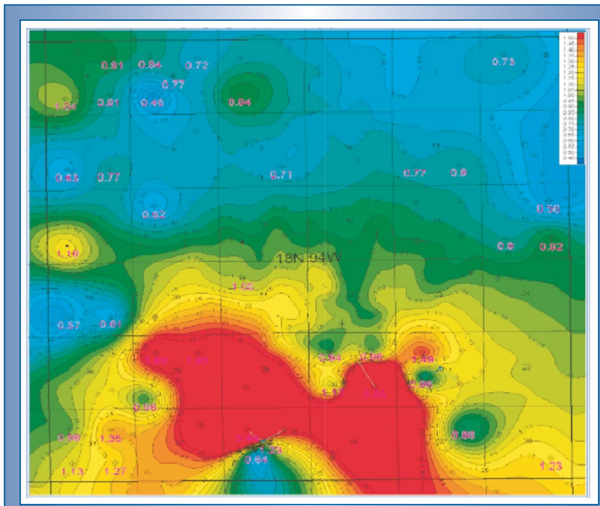

Figure 3. Resistivity of Almond formation produced water, normalized to 68°F where red areas are greater than 2 ohm-m, and blue areas are less than 0.6 ohm-m. It is relatively rare to see a four-fold variation in formation water resistivity. Recognition of an anomaly is the first step to resolving a problem.

capabilities, an interpreter can easily segregate the data geographically, establish correlations and perform transforms to create maps of interest. For example, resistivity of produced waters has not always been measured or recorded. The digital database allows a relationship to be constructed between a commonly available attribute, total dissolved solids (TDS) and resistivity (Figure 2). This relationship can then be used to estimate resistivity for samples where the attribute was not originally measured and mapped to explore potential geographic relationships (Figure 3).

The historical water chemistry data often was collected from more limited intervals than are commonly completed today. This detailed data, together with TDS, core data, production data and petrophysical advances can significantly improve completion efficiency by allowing the operator to have greater confidence in local pay criteria. Use of valid existing analytical data can save thousands of dollars in acquisition or completion costs.

The historical water chemistry data is an invaluable tool in exploration programs. Formation water compositional data from existing wells supports updated petrophysical interpretations in search of bypassed pay and regional diagenetic interpretations. Figure 4 is a chart of calcite saturation indices derived from the database. The Table Rock and Standard Draw areas are under-saturated in calcite when compared with the other producing areas sampled. Under-saturation of calcite could be an indicator of active calcite dissolution and creation of secondary porosity in the reservoirs. Such information also would be valuable in evaluating the extent of cementation in naturally fractured reservoirs. Both strategies could be used to focus exploration efforts in the search for above average permeability in low-permeability reservoirs.

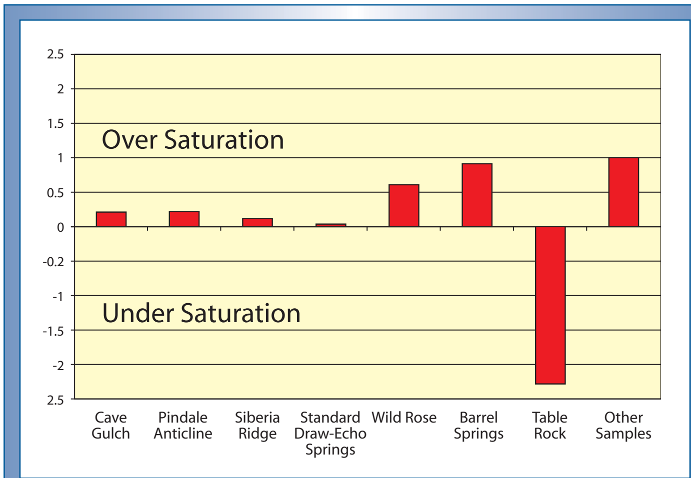

Figure 4. Chart of calcite saturation indices for eight areas in the Greater Green River Basin (GGRB) where positive is over-saturated and negative is under-saturated. Calcite is a common constituent of Cretaceous reservoirs in the GGRB. Reservoirs where waters are under-saturated in calcite could be expected to have a higher proportion of secondary porosity and/or less calcite fracture fill.

Water chemistry is an underutilized tool that can improve reservoir understanding and reduce risk when exploring and developing tight gas resources. Availability of this large produced water chemistry data collection in digital form facilitates efficient identification, extraction and utilization of the data by the technically-oriented, cost-conscious operator. ✧

Briefs

R&D Seeks to Bolster Coalbed Gas, Water Resources in Western States

U.S. Department of Energy-funded research has resulted in the commercialization of an innovative technology designed to bolster supplies of two of America's most critical natural resources: natural gas and water. The technology, developed by Drake Engineering of Helena, Mont., helps producers of coalbed natural gas (CBNG) clean up co-produced water for beneficial uses, in turn addressing critical water shortages in the U.S. West. Such research answers President George W. Bush's call for expanding domestic oil and gas production while protecting the environment. CBNG-produced water presents unique challenges for recovering this resource. Some landowners and environmental groups worry the water used in irrigation or discharged onto the land could alter the soil's structure and chemistry – a particular concern for crop irrigation. Drake Engineering designed and developed a prototype of a lab-tested fluid-bed resin exchange treatment system for removing sodium from CBNG-produced water. Drake has patented and begun commercializing the process by field-testing it in Powder River Basin CBNG operations. *www.netl.doe.gov/publications/press/2005/tl_coalbed_gas.html*

Events

AAPG Eastern Meeting

Sept. 18-20, Morgantown, W. Va. For more information, visit *www.wvgs.wvnet.edu/www/esaapg05/*

IOGCC Annual Meeting

Sept. 18-20, Jackson Hole, Wyo. For more information, visit *www.iogcc.state.ok.us*

Publications

Mapping Gas Reservoirs using Seafloor EM Methods

Gas reservoirs are electrically resistive compared with water saturated surrounding sediments. Marine electromagnetic (EM) methods have become important tools in the search for oil and gas. This report documents the use of marine EM methods to identify and map reservoirs through computer model studies. The marine magnetotelluric (MT) method and the controlled source electromagnetic (CSEM) method combine complementary abilities to map the electrical conductivity structure of oilfield rocks and reservoirs. This project created 2-D and 3-D forward modeling codes based on the finite element and finite difference algorithms by creating accessible front-end user interfaces for these codes and generating joint MT and CSEM data sets relevant to the exploration environment. The work described in this report represents the first steps toward the development of a fully 3-D finite element forward code allowing rapid and accurate EM modeling of marine geophysical targets. In addition, a joint controlled-source EM and MT data set was prepared as a test-bed to develop forward and inverse modeling algorithms. The Gemini prospect in the Gulf of Mexico has been a test-bed for the development of commercial EM instrumentation and techniques, and a comprehensive MT and CSEM data set has been developed over this 3-D salt structure that will be available for modeling. Price: $60, Form: CD-ROM, Document No: GRI-04/0200. Order through the Gas Technology Institute Web site "search" function at *www.gastechnology.org*

Conceptual Design for a Large-Diameter Gas Pipeline Inspection Platform

A final report is available that presents the conceptual design of an intelligent platform for internal pipeline examination. The design is a result of balancing power requirements, battery size and physical restraints to develop a vehicle that can handle high-pressure environments, long distance, vertical travel and various protruding obstacles. The final multi-wheel configuration allows the vehicle to navigate vertical sections, travel up inclines and spiral its position in the pipe to avoid obstacles while minimizing power requirements and sources of friction. *www.netl.doe.gov/scngo/NaturalGas/Projects_n/TD&S/T&D/Pubs/4340-70A_Conceptual%20Design%20Final.pdf*

Very High-Speed Drillstring Communications Network

A final report is available providing a history and project summary of the development of a very high-speed drillstring communications network. The summary includes laboratory and field test results. A brief explanation of commercialization plans is included. This work shows that a high data rate communications system can be made sufficiently robust, reliable and transparent to the end user to be successfully deployed in a downhole drilling environment. A networking system with user data bandwidth of at least 1 million bits per second can be built to service any practical depth of well using multiple repeaters (Links), with spacing between the links of at least 1000ft. *www.netl.doe.gov/scngo/NaturalGas/Projects_n/E&P/DCS/Pubs/Final%20Report%20FG123104.pdf*

Liquefied Natural Gas: Understanding the Basic Facts

A report prepared by the U.S. Department of Energy in collaboration with the National Association of Regulatory Utility Commissioners is available that discusses growing demand for natural gas, emergence of the global liquefied natural gas (LNG) market, current status of U.S. LNG imports, components of the LNG value chain and informed decision making. *www.netl.doe.gov/scngo/NaturalGas/publications/LNG/LNG_BasicFacts.pdf*

Contact Information

Gas Technology Institute (GTI)
1700 S. Mount Prospect Road
Des Plaines, IL 60018-1804
Phone: (847) 768-0500; Fax: (847) 768-0501
E-mail: *publicrelations@gastechnology.org*
Web site: *www.gastechnology.org*

GTI E&P Research Center
1700 S. Mount Prospect Road
Des Plaines, IL 60018-1804
Phone: (847) 768-0500; Fax: (847) 768-0501
E-mail: *explorationproduction@gastechnology.org*
Web site: *www.gastechnology.org*

GTI/Catoosa℠ Test Facility, Inc.
19319 N. E. 76th, Owasso, OK 74015
Phone: Toll-free (877) 477-1910
Fax: (918) 274-1914
E-mail: *srandolph@gticatoosa.org*

U.S. Department of Energy
National Energy Technology Laboratory
Web site: *www.netl.doe.gov/scngo*

3610 Collins Ferry Road
Morgantown, WV 26507-0880

626 Cochrans Mill Road
Pittsburgh, PA 15236-0340

One W. Third St.
Tulsa, OK 74103-3519

525 Duckering
Fairbanks, AK 99775

Office of Fossil Energy
1000 Independence Ave., S.W.
Washington, DC 20585
Web site: *www.fe.doe.gov*

NETL gti HART